

## Transmission through barriers and resonant tunneling in an interacting one-dimensional electron gas

C. L. Kane

*Department of Physics, University of Pennsylvania, Philadelphia, Pennsylvania 19104*

Matthew P. A. Fisher

*Institute for Theoretical Physics, University of California, Santa Barbara, California 93106  
and IBM Research, Thomas J. Watson Research Center, P.O. Box 218, Yorktown Heights, New York 10598*

(Received 10 June 1992)

We study theoretically transport of a one-dimensional single-channel interacting electron gas through barriers or constrictions. We find that electrons with repulsive interactions, incident upon a single barrier, are completely reflected at zero temperature. At finite temperature ( $T$ ), the conductance is shown to vanish as a power of  $T$ , and at zero temperature, power-law current-voltage characteristics are predicted. For attractive interactions, we predict perfect transmission at zero temperature, with similar power-law corrections. We also study resonant tunneling through a double-barrier structure and related effects associated with the Coulomb blockade. Resonant peaks in the transmission are possible, provided the interactions are not too strongly repulsive. However, in contrast to resonant tunneling in a noninteracting electron gas, we find that in the presence of interactions the width of the resonance vanishes, as a power of temperature, in the zero-temperature limit. Moreover, the resonance line shapes are shown to be described by a universal scaling function, which has power law, but non-Lorentzian tails. For a particular choice of interaction strengths, we present an exact solution of our model, which verifies the scaling assumptions and provides an explicit expression for the scaling function. We also consider the role played by the electron-spin degree of freedom in modifying the transmission through barriers. With spin, there are four possible phases corresponding to perfect transmission or perfect reflection of charge and spin. We present phase diagrams for these different behaviors and analyze the nontrivial transitions between them. At these transitions we find that the conductance or transmission is universal—depending only on the dimensionless conductance of the leads and not on the details of the barriers. In the case of resonant tunneling with spin, we discuss the “Kondo” resonance, which occurs when there is a spin degeneracy for electrons between the two barriers. Many of the predictions should be directly testable in gated GaAs wires.

### I. INTRODUCTION

Since the discovery of the high-temperature superconductors<sup>1</sup> there has been a resurgence of interest in strongly correlated electron systems. Due to the strange normal-state properties of these materials, much attention has focused on strongly interacting electron models with a view to finding some which exhibit non-Fermi-liquid-like normal phases.<sup>2</sup> A paradigm for such non-Fermi-liquid behavior can be found in one-dimensional (1D) interacting electron models, in which the Fermi surface is altered *qualitatively* even for weak interactions. Indeed, it is well established theoretically<sup>3–7</sup> that the low-temperature properties of such interacting 1D models are described in terms of a Luttinger liquid, rather than a Fermi liquid. Despite the firm foundation upon which the Luttinger liquid rests in 1D, its possible relevance to 2D or 3D strongly interacting electron systems remains unclear. In view of this, it seems worthwhile to first search for Luttinger-liquid behavior experimentally in electron systems which are one dimensional.

Fortunately, in very recent years it has become possi-

ble, by cleverly gating 2D electron gases in GaAs inversion layers, to make truly one-dimensional “wires.”<sup>8,9</sup> Due to the low carrier concentration these wires can be made so narrow as to carry only several, or even one, transverse channel. Moreover, since the mobility in GaAs can be very large, it is possible that localization effects, which will eventually dominate in a long enough wire, can be effectively minimized. In such systems transport measurements should be possible and might give evidence for Luttinger-liquid behavior. In view of this possibility, it is rather surprising how little theoretical effort has focused on transport properties of Luttinger liquids.

In this paper we summarize our recent theoretical work studying transport in an interacting 1D electron gas. With a view toward possible experiments, we focus on the case where the transport is through one, or perhaps two, weak links or constrictions. Such constrictions can be fabricated by adding additional gates to the system. Our underlying physical assumption is that the rest of the 1D wire is sufficiently clean that the resistance of the wire is dominated by the transport through the constrictions. Indeed, we will ignore completely disorder

in the rest of the wire, and focus exclusively on the transmissions and reflections from the constrictions. Experimentally, it may be easiest to eliminate unwanted scattering from impurities in the one-dimensional channel by working in a strong magnetic field, which will tend to spatially separate the right and left moving electrons. The optimal separation is achieved when the magnetic length is approximately equal to the width of the “wire” in which the electrons are confined.

Since any wire will be of finite length, and in a transport experiment one must connect the wire to three-dimensional leads, care must be taken to ensure that it is the one-dimensional physics of the wire rather than the three-dimensional physics of the leads which is being probed. We shall see that this will be the case provided the wire is longer than a thermal coherence length  $L_T = \hbar v_F / k_B T$ , where  $v_F$  is the Fermi velocity. Alternatively, for a fixed length wire, one must work at a temperature larger than  $T_L = \hbar v_F / k_B L$ . In GaAs with a density of one electron per 10 nm, a 1- $\mu\text{m}$ -long wire would correspond to a temperature  $T_L = 10$  mK.

Even in a wire with no constrictions, the “two-terminal” conductance for a single-channel interacting electron gas is *not* given by  $e^2/h$  as it is in a Fermi liquid of noninteracting electrons. To see why this is so, recall the usual argument for quantization of the conductance of a single-channel wire.<sup>10</sup> If the left and right leads of the wire are in equilibrium with reservoirs at chemical potentials separated by eV, then there will be an excess of  $\kappa$  eV/2 states carrying current away from the reservoir at higher chemical potential. Here  $\kappa = \partial n / \partial \mu$  is the compressibility. The current carried by each state is determined by the velocity  $ev_F$ . The remarkable quantization of the conductance,  $G = e^2/h$ , then follows from the special relationship between the Fermi velocity and the compressibility for 1D noninteracting electron gas,  $\kappa v_F = 1/(\pi \hbar)$ . For interacting electrons, both the compressibility and the velocity are renormalized, and this cancellation need no longer precisely occur. Therefore, if we define  $g = \pi \hbar \kappa v$ , then the conductance is given by  $G = ge^2/h$ . The dimensionless parameter  $g$  is a measure of the strength of the interactions and plays a central role in the theory. For the case of spinless electrons, relevant to experiments in strong magnetic fields, the noninteracting value for  $g$  is 1, and for repulsive interactions (which decrease the compressibility),  $g$  is less than 1 and given roughly by the expression  $g^2 \approx (1 + U/2E_F)^{-1}$ . Here  $U$  is the Coulomb interaction between neighboring electrons and  $E_F$  is the Fermi energy. The ratio  $U/E_F$  is proportional to  $r_s$ , the electron spacing divided by the Bohr radius, so that  $g$  decreases with decreasing electron density. Thus, in GaAs, where the carrier concentration is much lower than in a metal,  $g$  can be appreciably smaller than 1, say in the range  $\frac{1}{8} - \frac{1}{2}$ . This reflects the enhanced role that electron interactions play at low densities.

For electrons with spin, we denote the dimensionless (two-terminal) conductance by  $g_\rho$ . For interacting electrons we have  $g_\rho = 2$ , coming from the spin-up and spin-down electrons, whereas for repulsive interactions  $g_\rho < 2$ . In addition, for electrons with spin, one may define a

“spin conductance”  $G_\sigma$  via the spin-current response to a graded magnetic field. We define a dimensionless “spin conductance” as  $G_\sigma = g_\sigma e^2/h$ . For noninteracting electrons,  $g_\sigma = 2$ . Moreover, we shall see that in the absence of a magnetic field or spin-dependent scattering,  $g_\sigma = 2$  even in the presence of interactions. While the spin conductance is more difficult to measure than the charge conductance, it also will play a central role in our theory.

The difference between a single-channel interacting Luttinger liquid and a noninteracting Fermi liquid is far more spectacular in the presence of a single narrow constriction. According to Landauer transport theory,<sup>10</sup> the conductance of a single-channel wire with a barrier is determined by the transmission probability through the barrier for a wave incident from one of the leads. The conductance may vary continuously between 0 and  $e^2/h$ . The underlying assumption of Landauer theory is that the electrons in the leads may be adequately described with noninteracting electrons. This is usually the case for a Fermi liquid. In one dimension, however, electron-electron interactions play a crucial role, and the Fermi surface is destroyed.<sup>5</sup> In a Luttinger liquid, the interactions dramatically alter the effects of barriers on transport. In particular, we show that at  $T = 0$ , a repulsively interacting Luttinger liquid is *completely* reflected from even the smallest of barriers, and the conductance through the constriction is zero. At finite temperature the conductance through the constriction is finite, and is found to vanish as a power of temperature,

$$G(T) \approx T^{2/g-2}. \quad (1.1)$$

For electrons with spin,  $2/g$  is replaced by  $2/g_\rho + 2/g_\sigma$ . At zero temperature, a similar power-law behavior is found in the frequency dependence of the conductivity. Moreover, the dc  $I$ - $V$  characteristics are predicted to be non-Ohmic, and have the form

$$I(V) \approx V^{2/g-1}. \quad (1.2)$$

At low temperatures and voltages, this power-law behavior will be cut off in a finite length wire by the energy scale  $T_L$ . Thus we only expect (1.1) and (1.2) to be valid for energy scales larger than  $T_L$ . Below that, there will be Ohmic conductance with  $T$  replaced by  $T_L$  in (1.1).

Physically, we may interpret the insulating behavior of a single barrier with repulsive interactions in the following way. In a Luttinger liquid, there is a tendency towards charge-density-wave (CDW) order. Of course, there can be no true long-range order in one dimension, but it is well known that the CDW correlations decay *algebraically* in space and time with an exponent which decreases as  $g$  decreases.<sup>5</sup> For  $g < 1$ , or repulsive interactions, these correlations are long range enough so that an arbitrarily weak barrier will pin the incipient charge-density wave at low energies.

For attractive interactions, on the other hand, we predict *perfect transmission* through an arbitrarily large barrier at zero temperature with similar power-law corrections at finite  $T$ ,  $\omega$ , or  $V$ . Heuristically, the superconducting correlations are sufficiently long range, and the phase difference across the junction is “pinned” by an arbitrari-

ly weak coupling.

Next we consider the problem of resonant tunneling through a double-barrier structure. This situation is particularly interesting in light of recent experiments in which oscillations in the conductance through a double constriction have been observed as a function of the chemical potential.<sup>8</sup> These oscillations are believed to correspond to the addition of single electrons to the “island” between the two constrictions, and to be a result of the Coulomb blockade,<sup>11,12</sup> which forbids tunneling onto the island unless the chemical potential is tuned to a value where another electron can be added with no cost in energy.<sup>13</sup> In this situation electrons may resonantly tunnel through the island.

A great deal of attention has been focused lately on the effects of the Coulomb interactions on the island, which lead to the Coulomb blockade.<sup>14</sup> However, as we show, in addition, the electron-electron interactions in one-dimensional leads play a crucial role. Despite the fact that a single narrow constriction causes total reflection, we show that a Luttinger liquid incident on a double-barrier structure can exhibit perfect resonant transmission. When the barriers are symmetric, this resonance may be achieved by tuning a single parameter, such as a gate voltage. More generally, however, for asymmetric barriers, two parameters must be tuned to achieve resonance. Moreover, when the electron-electron interactions are stronger than a critical value (which could be the case when the electron density is very low) then even more parameters need to be tuned in order to achieve resonance. In this case, such “higher-order” resonances would be more difficult to observe.

For a wire modeled by noninteracting electrons, the shapes of these resonance peaks should be Lorentzian at low temperatures, with a temperature-independent width. In contrast, we find that when the electrons in the one-channel wire are interacting, i.e., in a Luttinger liquid, the resonance peaks (as a function of gate voltage, for instance) are *infinitely sharp* at zero temperature. At low but nonzero temperatures, the resonances develop a width which vanishes as a power of temperature. If we denote the “distance” to the resonance in gate voltage by  $\delta$ , then the conductance through the resonance at low temperatures is predicted to have a universal shape described by a scaling function:

$$G(T, \delta) = \tilde{G}(\delta/T^\lambda). \quad (1.3)$$

The scaling function  $\tilde{G}(X)$  and the exponent  $\lambda$  are universal in the sense that they depend only on the lead conductances and not on the details of the barriers. In general  $\tilde{G}(X)$  has power-law but non-Lorentzian tails.

The above results, which are primarily established by piecing together perturbative calculations with scaling ideas, are confirmed and strengthened by an exact solution for the spinless case when  $g = \frac{1}{2}$ . Abridged versions of some of these results have been reported previously in Refs. 15 and 16.

In this paper we also generalize our results to include a spin degree of freedom for the electrons. When there is an SU(2) spin symmetry, our results for a single barrier are quite similar to the spinless case. Namely, we expect

a perfectly insulating link for repulsive interactions and a perfectly conducting link for attractive interactions. More generally, however, in the presence of spin it is possible to have two additional phases in which either charge is perfectly transmitted and spin is reflected, or spin is perfectly transmitted and charge is reflected. Under certain conditions, which we will specify below, these “mixed phases” will be stable.

Resonant tunneling is also possible with a spin degree of freedom, and again, at low temperatures, the resonance line shapes will be described by a scaling function similar to (1.3). The interpretation of these resonances in the Coulomb blockade regime is rather different, though. When the number of electrons on the central island is given by an odd integer, there is an excess spin on the island. This is reminiscent of the Kondo problem in which a spin- $\frac{1}{2}$  local moment is coupled to conduction electrons. It has been suggested that for Fermi-liquid leads, there can be a Kondo effect in which the spin on the island is compensated by the electrons in the leads by the formation of a resonant bound state at the Fermi energy.<sup>17–19</sup> In this case, perfect resonant transmission is predicted for a symmetric barrier. We find that these Kondo-like resonances are also present in the interacting Luttinger liquid. As in the noninteracting case, we find perfect transmission on resonance, although with interactions the resonance becomes infinitely sharp in the zero-temperature limit. In general, these Kondo resonances can be achieved by tuning two parameters, but for a symmetric (double) barrier, only a single parameter, for example, a gate voltage, is needed. It should be emphasized that these Kondo resonances are qualitatively different than the resonances that occur in the spinless electron gas. In the case without spin, the resonance condition corresponds to tuning to a degenerate charge state on the island. At the Kondo resonance, by contrast, there is a degenerate spin state on the island, with only virtual charge fluctuations allowed.

Our paper is organized as follows. In Sec. II we review the properties of a pure Luttinger liquid and compute its two-terminal conductance. In Sec. III we discuss transport through a single barrier for spinless electrons. We are able to do perturbative calculations in the extreme limits of very weak barriers and very weak tunneling, and join these two regimes using renormalization-group arguments. In Sec. IV we perform a similar analysis of resonant tunneling through a double-barrier structure, and present the phase diagram for transmission precisely on resonance. In Secs. V and VI we generalize the results of Secs. III and IV to include a spin degree of freedom. Section V is devoted to an analysis of transmission through a single barrier, whereas resonant transmission through a double-barrier structure for the spinful case is discussed in Sec. VI. In Sec. VII we address the resonance line shapes at finite temperature and argue that their temperature dependence is described by a universal scaling function. In Sec. VIII we confirm this explicitly with an exact solution of our model for the special case  $g = \frac{1}{2}$ . Finally, Sec. IX is devoted to a discussion of various relevant experimental and theoretical questions and concluding remarks.

## II. THE LUTTINGER LIQUID

The defining feature of a Fermi liquid is the discontinuity at the Fermi surface of the electron momentum density of states. In one dimension, it has been established theoretically that electron-electron interactions destroy this discontinuity and replace it by a power-law nonanalyticity at the Fermi surface.<sup>3-5</sup> The ground state of the interacting one-dimensional electron gas in the absence of any scattering potentials is a "Luttinger" liquid.<sup>6</sup> This state is characterized by a gapless collective sound mode, and has physical correlation functions which decay algebraically in space and time with exponents which depend continuously on the interaction strength.

The electron-electron interactions in one dimension may be treated using perturbative renormalization-group methods, which leads to the so-called "g-ology" theory.<sup>5</sup> It is found that in the absence of backward scattering a system of spinless electrons can be described at low energies and long length scales by a line of (renormalization-group) fixed points characterized by a single parameter  $g$ . This parameter depends continuously on the strength of the electron-electron interaction (which has been assumed to be of short range). Depending on  $g$ , backwards scattering (via umklapp or impurity scattering) may or may not be relevant perturbation on these Luttinger-liquid fixed points. In this paper, we confine our interest to the case of electrons off lattice, or when on lattice well away from half-filling, so that umklapp scattering is not important. Furthermore, when considering an electron gas with spin, we assume the system is well away from spin-density-wave and superconducting instabilities.

A particularly simple way of describing the low-energy physics of a Luttinger liquid is via the method of "bosonization."<sup>5</sup> Although this is a standard method which has been well studied, for completeness we briefly review its ingredients following a procedure originally due to Haldane.<sup>7</sup> For spinless electrons, we perform a Jordan-Wigner transformation, which represents the fermion creation operator in terms of a hard-core boson,  $c_i^\dagger \rightarrow \exp(i\pi \sum_{j<i} n_j) b_i^\dagger$ . The interacting bosons are then represented in the number-phase representation  $b_i^\dagger = \sqrt{n_i} \exp(i\chi_i)$ . In the continuum limit, we define bosonic fields  $\theta$  and  $\phi$  such that  $n_i \rightarrow \bar{\rho} + \nabla\theta(x)/\sqrt{\pi}$  and  $\chi_i \rightarrow \sqrt{\pi}\phi(x)$  ( $\bar{\rho} = k_F/\pi$  is the mean density). It then follows from the canonical commutation relation between number and phase that  $\theta$  and  $\phi$  satisfy

$$[\phi(x), \theta(x')] = -i\Theta(x-x'). \quad (2.1)$$

Thus  $\nabla\theta(x)$  may be regarded as the momentum conjugate to  $\phi(x)$ . Alternatively,  $\nabla\phi(x)$  is the conjugate momenta to  $\theta$ . Expressed in terms of these bosonic fields, the fermion field operator may be written

$$\psi^\dagger(x) \approx \sum_{n \text{ odd}} \exp\{in[\sqrt{\pi}\theta(x) + k_F x]\} \exp[i\sqrt{\pi}\phi(x)]. \quad (2.2)$$

The sum on  $n$  enforces the constraint that the particle density be discrete. By having  $n$  odd, the Jordan-Wigner string is included and Fermi statistics is obeyed. We ig-

nore the  $\nabla\theta$  terms which arise from expanding  $\sqrt{n}$ , since they will be irrelevant at long wavelengths. In other formulations of bosonization<sup>5,6</sup> only the  $n = +1$  and  $-1$  terms in the sum are included, corresponding to right and left moving pieces of the electron. In general, though, higher-order terms in the sum are allowed by the symmetry  $\theta \rightarrow \theta + \sqrt{\pi}$  (which represents the discrete particle nature of the electrons), and if not included explicitly in (2.2) must be included (whenever important) in the effective Lagrangian (see Sec. III).

The interactions between these bosons result from a combination of the hard-core constraint and the electron-electron interactions in the original fermion problem. Provided these interactions are short ranged, the effective Hamiltonian at long wavelengths may be written in the generic form

$$H = v \left[ \frac{g}{2} (\nabla\phi)^2 + \frac{1}{2g} (\nabla\theta)^2 \right]. \quad (2.3)$$

Here  $v$  is the sound velocity, and the parameter  $g$  decreases with increasing repulsion, but depends in a complicated way on the microscopic parameters of the problem. However, as we shall see, it is directly related to the compressibility of the system, and  $g = 1$  describes the noninteracting Fermi gas.

By passing from Hamiltonian to Lagrangian in either  $\phi$  or  $\theta$  we may obtain two equivalent descriptions of the Luttinger liquid. These may be expressed in terms of the Euclidean action

$$S = \int dx d\tau \frac{v}{2g} \left[ (\nabla\theta)^2 + \frac{1}{v^2} (\partial_\tau\theta)^2 \right] \quad (2.4a)$$

$$S = \int dx d\tau \frac{vg}{2} \left[ (\nabla\phi)^2 + \frac{1}{v^2} (\partial_\tau\phi)^2 \right]. \quad (2.4b)$$

We refer to these dual representations as the  $\theta$  representation and the  $\phi$  representation.

Equations (2.4a) and (2.4b) may be understood more physically with the following heuristic description. In one dimension, the fluctuations about a Wigner crystal state may be described using a set of phonon coordinates which represent the displacement of the electrons from their lattice positions. If we denote this displacement by  $\theta a/\sqrt{\pi}$  ( $a$  is the mean electron separation), then the density (fluctuations) and the current will be given by  $\sqrt{\pi}\nabla\theta$  and  $\sqrt{\pi}\partial_\tau\theta$ , respectively. Equation (2.4a) then simply describes the long-wavelength phonon fluctuations. In one dimension, the quantum fluctuations of these modes destroy the long-ranged crystalline order, and one is left with algebraically decaying positional correlations even at  $T=0$ . This is manifested in a logarithmic divergence in the Debye-Waller factor. It is clear that the parameters  $v$  and  $g$  in (2.4a) depend only on  $m^*$  (the effective electron mass),  $a$ , and the compressibility  $\kappa$ :  $g = \pi\hbar\sqrt{\kappa}/ma$ ,  $v = \sqrt{1/\kappa ma}$ . In particular, the relation  $g = \pi\hbar\kappa v$  alluded to in the Introduction is satisfied. For noninteracting electrons, we thus have  $g = 1$ .

The dual  $\phi$  representation (2.4b) can be understood heuristically in terms of the phase of the boson field ( $b$ ) introduced in the Jordan-Wigner transformation.

Specifically, (2.4b) describes the phonon modes of the boson superfluid phase. Again, the quantum fluctuations in one dimension destroy the long-range order, leaving algebraically decaying superfluid correlations at  $T=0$ . While heuristic in nature, these two pictures do provide a useful guide in understanding the effects of scattering potentials studied below.

The above considerations may be generalized to include a spin degree of freedom by defining a boson field  $\theta_\mu$  and  $\phi_\mu$  for each species of electron,  $\mu = \uparrow, \downarrow$ . The fermion field operators  $\psi_\mu(x)$  may be expressed in terms of  $\theta_\mu$  and  $\phi_\mu$  as in (2.2). It is convenient to introduce new boson fields for the charge and spin degrees of freedom, denoted by subscripts  $\rho$  and  $\sigma$ , for both  $\theta$  and  $\phi$ :

$$\theta_\rho = \theta_\uparrow + \theta_\downarrow, \quad (2.5a)$$

$$\theta_\sigma = \theta_\uparrow - \theta_\downarrow, \quad (2.5b)$$

and

$$\phi_\rho = (\phi_\uparrow + \phi_\downarrow)/2, \quad (2.6a)$$

$$\phi_\sigma = (\phi_\uparrow - \phi_\downarrow)/2. \quad (2.6b)$$

In terms of these fields, the Euclidean action describing the Luttinger liquid will have the generic form

$$S = \int dx d\tau \frac{v_\rho}{2g_\rho} \left[ (\nabla\theta_\rho)^2 + \frac{1}{v_\rho^2} (\partial_\tau\theta_\rho)^2 \right] + \frac{v_\sigma}{2g_\sigma} \left[ (\nabla\theta_\sigma)^2 + \frac{1}{v_\sigma^2} (\partial_\tau\theta_\sigma)^2 \right]. \quad (2.7a)$$

Similarly, in the  $\phi$  representation,

$$S = \int dx d\tau \frac{v_\rho g_\rho}{2} \left[ (\nabla\phi_\rho)^2 + \frac{1}{v_\rho^2} (\partial_\tau\phi_\rho)^2 \right] + \frac{v_\sigma g_\sigma}{2} \left[ (\nabla\phi_\sigma)^2 + \frac{1}{v_\sigma^2} (\partial_\tau\phi_\sigma)^2 \right]. \quad (2.7b)$$

With spin, noninteracting electrons correspond to  $g_\rho = g_\sigma = 2$ . Moreover, in the absence of a magnetic field or any spin-dependent interactions, one must take  $g_\sigma = 2$  in order to respect the underlying SU(2) spin symmetry. More generally, an additional magnetic interaction term of the form  $uS_i^+ S_i^- \rightarrow u \cos(2\sqrt{\pi}\theta_\sigma)$  is allowed. However, for repulsive electron-electron interactions the ‘‘bare’’ value of  $g_\sigma < 2$ , so that this term is irrelevant at long wavelengths, and the system flows to the fixed point described by (2.7) with renormalized values  $u=0$  and  $g_\sigma=2$ .<sup>20</sup> For attractive electron interactions, however, this term is relevant, reflecting the instability towards  $s$ -wave singlet superconductivity, and opens up a gap in the spin part of (2.7), rendering  $\theta_\sigma$  massive. In this paper we will focus primarily on the case with the  $g_\sigma=2$  case, but our results will also be valid when  $g_\sigma < 2$  provided the parameters are such that  $u$  flows to zero.

The single-electron Green’s function  $G(x, \tau) = \langle T_\tau \psi^\dagger(x, \tau) \psi(0, 0) \rangle$  may be evaluated using (2.2)–(2.4).

For spinless electrons, we find

$$G(x, 0) \approx \sin(k_F x) x^{-(g+g^{-1})/2}, \quad (2.8)$$

where we have retained only the leading long-distance behavior which is dominated by the  $n = \pm 1$  terms in (2.2). For electrons with spin, the exponent is replaced by  $(g_\rho + g_\sigma)/8 + (g_\rho^{-1} + g_\sigma^{-1})/2$ . For a one-dimensional Fermi liquid we expect  $G(x, 0) \approx 1/x$ . We can thus confirm that  $g = 1$  corresponds to the case of noninteracting electrons (or  $g_\rho = g_\sigma = 2$  with spin). For  $g \neq 1$ , a larger power is found, which implies that the Fermi surface discontinuity is reduced to a power-law nonanalyticity. It follows that the tunneling density of states  $\rho(\epsilon)$  vanishes upon approaching the Fermi energy as  $\rho(\epsilon) \approx \epsilon^{(g+1/g)/2-1}$  for spinless electrons.

It is well known that for noninteracting electrons the two-terminal conductance of a 1D wire with no elastic scattering is  $e^2/h$  per channel. In the Introduction we argued that for interacting electrons, this should be replaced by  $ge^2/h$ . This may be confirmed by an explicit calculation of the two-terminal conductance. We follow the procedure implemented by Fisher and Lee,<sup>21</sup> which involves calculating the current in linear response to an electric field  $E = V/L$  applied to a finite region of length  $L$  of an infinitely long wire. At zero temperature this is accomplished by computing the current-current correlation function:

$$G = \lim_{\omega \rightarrow 0} \frac{1}{\hbar L \omega} \int dx d\tau e^{i\omega\tau} \langle T_\tau J(x, \tau) J(0, 0) \rangle, \quad (2.9)$$

where the current  $J(x, \tau) = ie\partial_\tau\theta(x, \tau)/\sqrt{\pi}$  and the integration over  $x$  is restricted to the region of length  $L$ . Evaluating (2.9) using (2.4) we find that for a pure Luttinger liquid

$$G = g \frac{e^2}{h}. \quad (2.10)$$

As was originally shown by Apel and Rice,<sup>22</sup> we see that the ‘‘rule’’ of  $e^2/h$  conductance per channel is modified in the presence of interactions. For electrons with spin,  $g$  is replaced by  $g_\rho$ . Thus, we may interpret  $g$  and  $g_\rho$  to be dimensionless measures of the conductance of the pure Luttinger liquid. An identical calculation for the spin ‘‘conductance’’ reveals that  $G_\sigma = g_\sigma e^2/\hbar$ .

While it is difficult to determine precise values of  $g$  or  $g_\rho$  for a given microscopic model, they may be estimated by ‘‘correcting’’ the compressibility of the noninteracting electron gas to account for interactions. Specifically, we can add a Coulomb interaction  $U$  to the inverse compressibility, which leads to

$$g \approx \left[ 1 + \frac{U}{2E_F} \right]^{-1/2}. \quad (2.11)$$

Here  $U$  is of order  $e^2/\epsilon a$ , where  $a$  is the average spacing between electrons and  $\epsilon$  is an appropriate dielectric constant. The ratio  $U/2E_F$  is proportional to  $r_s = a/a_0$ , where  $a_0$  is an appropriate Bohr radius, and hence increases with decreasing density. Glazman, Ruzin, and Shklovskii<sup>23</sup> have made a more detailed estimate of

$U/2E_F$  in the situation where the long-range Coulomb interaction between the electrons is screened by a conducting plane a distance  $D$  away from the one-dimensional wire. They find  $U/2E_F \approx (2/\pi^2)\ln(8.0D/a)a/a_0$ .

### III. TRANSPORT OF SPINLESS ELECTRONS THROUGH A SINGLE BARRIER

In this section we discuss the effects of a single barrier on a gas of spinless electrons. As is well known, for the noninteracting electron gas an incident electron will be partially transmitted and partially reflected, with the relative amounts determined by the strength of the barrier. The conductance is given by the transmission probability times  $e^2/h$ . In this section we demonstrate that the presence of the electron-electron interaction has a profound and qualitative effect on such scattering. In the presence of interactions we can approach this problem perturbatively in two limits: A very weak barrier and a very large barrier (or equivalently weak tunneling), which we discuss below in Secs. III A and III B, respectively.

#### A. Weak barrier

Consider first the scattering of a pure Luttinger liquid from a small barrier. Specifically, we consider a potential scatterer  $V(x)$  which is nonzero only for  $x$  near zero, and whose maximum amplitude, taken to be at  $x=0$ , is small with respect to the Fermi energy. In terms of the electron field operator  $\psi(x)$ , the additional term we add to the electron Hamiltonian is simply,

$$\delta H = \int dx V(x) \psi^\dagger(x) \psi(x). \quad (3.1)$$

This can be expressed in terms of the boson field  $\theta$  by simply inserting the expression (2.2) into the above equation. Upon performing a gradient expansion in  $\theta(x)$  about  $x=0$ , performing the  $x$  integration and retaining only the most important terms we find a contribution to the Luttinger liquid action of the form

$$\delta S \approx \sum_{n=-\infty}^{\infty} \frac{1}{2} v_n \int d\tau e^{i2n\sqrt{\pi}\theta(x=0,\tau)}. \quad (3.2)$$

Here the coefficients  $v_n = v_{-n}^*$ , are proportional to the Fourier transform of  $V(x)$  at momenta given by  $n$  times  $2k_F$ :  $v_n = \hat{V}(2nk_F)$ . When the potential barrier has an inversion symmetry,  $V(x) = V(-x)$ , it follows that the  $v_n$  are real. Physically, this interaction corresponds to processes where  $n$  electrons are backscattered, each by a momenta  $2k_F$ , from one Fermi point to the other. Alternatively, (3.2) can be viewed as an effective potential  $V_{\text{eff}}[\theta(x=0)]$ , which is invariant under the transformation  $\theta \rightarrow \theta + \sqrt{\pi}$ . Since  $\theta/\sqrt{\pi}$  is the number of particles to the left of  $x=0$ ,  $V_{\text{eff}}$  may be regarded as a weak pinning potential in the Wigner crystal picture.

As we shall now see, for weak backscattering, the single-electron process, i.e., the  $2k_F$  backscattering term  $v_1$ , is the most important. Since the perturbation term above only acts at the origin,  $x=0$ , it is convenient to perform a partial trace in the partition function, and in-

tegrate out fluctuations in  $\theta(x)$  for all  $x$  away from zero. This is possible due to the quadratic nature of the pure Luttinger-liquid action (2.4). If we specify  $\theta(x=0,\tau) \equiv \theta(\tau)$ , then the action (2.4) is minimized when  $\theta(x,\omega_n) = \theta(\omega_n) \exp(-|\omega_n x|/v)$ , and the resulting effective action is

$$S_{\text{eff}} = \frac{1}{g} \sum_{\omega_n} |\omega_n| |\theta(\omega_n)|^2. \quad (3.3)$$

Notice the singular dependence on the Matsubara frequency  $\omega_n$ . If we Fourier transformed back to imaginary time  $\tau$ , this would correspond to a nonlocal interaction falling off as  $1/\tau^2$ . This interaction arises from the low-lying modes in the Luttinger liquid, and the coefficient is given by the inverse lead conductance  $g$ .

We are now in a position to perform a perturbative analysis to study the effect of the backscattering terms. Before undertaking a straightforward perturbation calculation for the conductance, we consider first a renormalization-group transformation. Specifically, after introducing a high-frequency cutoff,  $\Lambda$  in (3.3), which is roughly the Fermi energy, we imagine performing a partial trace over  $\theta(\omega)$  with  $\omega$  in the shell between  $\Lambda$  and  $\Lambda/b$ , with  $b > 1$ . The renormalization-group (RG) transformation is completed, as usual, by rescaling  $\tau' = \tau/b$ . We choose not to rescale the field  $\theta(\tau)$ , since then the quadratic action in (3.3) above is a fixed point of the RG transformation (i.e., the renormalized action is equivalent to the initial action with  $g$  unchanged). To leading order in the backscattering, the differential RG flow equations are determined by computing the dimension of the operator  $\cos 2n\sqrt{\pi}\theta$  and are

$$dv_n/dl = (1 - n^2 g)v_n, \quad (3.4)$$

where  $b = 1 + dl$ . The conductance  $g$  is not renormalized, to any order, since it is a coefficient of a singular operator ( $|\omega|$ ).

Notice that for attractive electron-electron interactions, where  $g > 1$ , all backscattering terms flow to zero (for any  $n$ ). For noninteracting electrons with  $g = 1$ , the  $2k_F$  backscattering is marginal, whereas all higher-order processes,  $4k_F$ ,  $6k_F$ , flow to zero. For repulsive interactions, though, the  $2k_F$  backscattering is always a relevant perturbation. That is, as one goes to lower energies under successive RG transformations, an initially weak  $2k_F$  backscattering grows stronger and stronger. As we will establish in Secs. III B and VIII below, this corresponds to total reflection at zero energy. A weak barrier is completely insulating for repulsive interactions. For attractive interactions, on the other hand, at low energies the barrier scales to zero and perfect transmission is expected.

It follows from the flow equations (3.4) that if we cut off the renormalization-group flows at some finite energy scale  $E$  (which could correspond to temperature, frequency, or voltage), then the effective barrier strength at that energy will be proportional to  $v_n E^{n^2 g - 1}$ . We thus anticipate power-law corrections to the conductance at finite temperature, frequency, or voltage. This can be confirmed by performing an explicit calculation of the

conductance perturbatively in  $V(2nk_F)$ . Some details of this calculation are outlined in Appendix A. At finite temperature  $T$ , we find to leading order in  $v_n$  that

$$G(T) = e^2/h \left[ g - \sum_{n=1}^{\infty} a_{nT} |v_n|^2 T^{2(n^2g-1)} \right], \quad (3.5a)$$

where  $a_{nT}$  is a dimensionful nonuniversal constant which depends, e.g., on the Fermi energy. At low temperatures the dominant correction will come from the term with  $n=1$ . Notice that for attractive interactions, where  $g > 1$ , as the temperature approaches zero the backscattering corrections to the conductance vanish. Although this has only been confirmed explicitly to second order in  $v_n$ , from the above RG analysis we expect it to hold even for large barriers (also see Sec. III B). For repulsive electron interactions the perturbation expansion breaks down as the temperature tends to zero, since the coefficient of the  $2k_F$  backscattering term ( $n=1$  term) diverges. This could have been anticipated from the RG approach. In Sec. III B we argue that in this case the electrons are completely reflected at  $T=0$ , even for a very weak barrier. For the special case of noninteracting electrons ( $g=1$ ) a nonzero backscattering reduction to the conductance survives down to  $T=0$ , as we know it must from a scattering analysis of the one-body Schrödinger equation in which part of the wave is transmitted and part is reflected.

Similarly, we may calculate corrections to the conductance at finite frequency and  $T=0$ ,

$$G(\omega) = e^2/h \left[ g - \sum_{n=1}^{\infty} a_{n\omega} |v_n|^2 \omega^{2(n^2g-1)} \right]. \quad (3.5b)$$

It is also possible to calculate the current-voltage characteristics as a perturbation expansion in the backscattering  $v_n$ . As shown in Appendix A, at  $T=0$  we find

$$I = Ve^2/h \left[ g - \sum_{n=1}^{\infty} a_{nV} |v_n|^2 V^{2(n^2g-1)} \right]. \quad (3.5c)$$

Once again, for repulsive interactions the  $2k_F$  backscattering contribution diverges in the small-voltage limit, vanishes for attractive interactions, and renormalizes the linear conductance for the noninteracting case. While the coefficients  $a$  are nonuniversal and depend on the form of the high-energy cutoff, their ratios are universal and are tabulated in Appendix A.

### B. Transport through a weak link

We now consider the opposite limit of a large barrier or equivalently a weak link (or tunnel junction). The zeroth-order problem in this limit is two completely disconnected semi-infinite leads. Here we analyze the effects of adding a small hopping matrix element  $t$  connecting the two leads. As in the previous section, we analyze the problem using a perturbative renormalization group.

A pair of disconnected semi-infinite Luttinger liquids may be described by inserting into the partition function, in the  $\theta$  representation (2.4a), a term of the form

$\delta[\theta(x=0, \tau)]$ . Since  $\theta(x=0, \tau)$  is essentially the number of particles to the left of  $x=0$ , this term effectively disconnects the two sides. For the purposes of this section, however, it is more convenient to work in the  $\phi$  representation, and in this case, it is equivalent to write the action for each side as

$$S_i = \int_0^\infty dx \int d\tau v \frac{g}{2} \left[ (\nabla\phi_i)^2 + \frac{1}{v^2} (\partial_\tau\phi_i)^2 \right], \quad (3.6)$$

where  $i$  refers to the  $+$  or  $-$  side of the barrier. Since the electron hopping term [(3.9) below] depends only on  $\phi(\tau) \equiv [\phi_+(x=0, \tau) - \phi_-(x=0, \tau)]/2$ , it is again convenient to integrate out all of the remaining quadratic degrees of freedom, namely  $\phi_\pm(x)$  for  $x$  not equal to zero. As in the previous section, we thereby arrive at an effective action for the weak link (or junction) of the form

$$S_{\text{eff}} = g \sum_{i\omega_n} |\omega_n| |\phi(\omega_n)|^2. \quad (3.7)$$

This action is precisely the dual of (3.3). It describes a fixed point under a renormalization-group transformation, and corresponds physically to a completely insulating tunnel junction.

A term which hops electrons across the weak link can be included in the original electron Hamiltonian by adding

$$\delta H \approx -t [\psi_^\dagger(x=0)\psi_-(x=0) + \text{H.c.}], \quad (3.8)$$

where  $t$  is an overlap matrix element. This may be simply expressed in terms of the field  $\phi$  by using (2.2):

$$\delta S = -t \int d\tau \cos 2\sqrt{\pi}\phi(\tau). \quad (3.9)$$

As in the previous section, we analyze the action (3.7) plus (3.9) with a renormalization-group analysis. In general, perturbations involving multiple electron hops will be generated, which take the form  $t_n \cos 2n\sqrt{\pi}\phi$ . (Note that from time-reversal invariance, it follows that a relative phase factor in the cosine term between the different  $n$ 's is not needed.) To leading order in  $t_n$  the RG flow equations are

$$dt_n/dl = (1 - n^2/g)t_n. \quad (3.10)$$

For repulsive electron-electron interactions ( $g < 1$ ) all of the  $t_n$ 's flow to zero, indicating that at low energies the junction is insulating. For attractive interactions,  $t_1$  grows under renormalization, and as we shall argue in the next section, ultimately flows to the pure Luttinger-liquid fixed point (with no backscattering) described in the previous section.

Some intuition for the flow equations (3.10) can be obtained by mapping the problem onto a 1D plasma of logarithmically interacting charges. This can be accomplished by formally expanding the exponential of the action (3.9) in the partition function in powers of  $t$ , and for each term integrating out  $\phi(\tau)$ . The resulting partition function is identical to that of a classical 1D statistical mechanics problem,

$$Z = \sum_n t^{2n} \sum_{q_i = \pm 1} \int_0^\beta d\tau_{2n} \cdots \int_0^\beta d\tau_1 \exp \left[ \sum_{i < j} V_{ij} \right], \quad (3.11a)$$



where

$$V_{ij} = \frac{2}{g} q_i q_j \ln(\tau_i - \tau_j) / \tau_c \quad (3.11b)$$

for  $\tau_i - \tau_j < \beta$ . The interacting charges ( $q_i = \pm 1$ ) have a simple physical interpretation: They are hopping events in which at time  $\tau_i$  an electron hops to the left or right across the junction.

The charges are positive (negative) for a hop to the right (left). The parameter  $t$  is essentially the fugacity of these charges, and the strength of their logarithmic interaction is  $2/g$ . This model is similar to that studied by Anderson, Yuval, and Hamman<sup>24</sup> in their study of the Kondo problem, however here there is no restriction on the sign of successive charges. For  $g < g_c = 1$ , the charges are bound, so that if an electron hops across the junction, it must eventually hop back, and the junction is insulating at long times or low energies. For  $g > 1$ , the interaction is effectively screened and free charges will be present, so that electrons are free to hop across the junction, and the junction conducts. The critical value  $g_c = 1$  may be deduced from the usual argument comparing the logarithmic cost in action of an isolated charge to the entropy gained.<sup>25</sup> A real-space RG procedure similar to that devised by Anderson, Yuval, and Hamann,<sup>24</sup> which will be used in Sec. IV, leads precisely to (3.10). It should be emphasized, though, that in contrast to the Kondo case, the coefficient of the logarithmic interaction  $g$  is not renormalized, which can be traced to the absence of a constraint on the sign of successive charges in (3.11).

The Coulomb gas model (3.11) is identical to an ‘‘instanton’’ representation of the partition function in the  $\theta$  representation (3.2) and (3.3), which is valid in the large- $v_n$  limit. To see this, note that for large  $v_n$ , there will be deep minima in the effective potential  $V_{\text{eff}}(\theta)$  which are related by the symmetry under  $\theta \rightarrow \theta + \sqrt{\pi}$ . At low energies, the partition function will be dominated by tunneling events (of  $\theta$  by  $\sqrt{\pi}$ ) between these minima (i.e., instantons). If we identify  $t$  with the fugacity of these instantons, then they will be described precisely by (3.11). It is in this sense that the  $\theta$  representation (3.2) and (3.3) is dual to the  $\phi$  representation, (3.7) and (3.9). This duality, which has been studied in detail in connection with the Caldeira-Leggett model of a resistively shunted Josephson junction,<sup>26,27</sup> will prove very useful in understanding the relationship between the small-tunneling (small- $t$ ) and small-backscattering (small- $v$ ) limits in the more complicated situation of resonant tunneling, which we treat in Sec. IV.

Finite temperature, frequency, or voltage will serve as a cutoff for the renormalization-group flows, and, as in the preceding section, we anticipate power-law corrections to the conductance. This may again be explicitly confirmed by a perturbative calculation to lowest order in the hopping strength  $t$ . As shown in Appendix A, the conductance at finite temperature may be written to leading order in small  $t$  as

$$G(T) = \sum_{n=1}^{\infty} b_n t_n^2 T^{2(n^2/g-1)}. \quad (3.12a)$$

Consistent with the RG flows (3.10), we find that for

repulsive interactions ( $g < 1$ ), the conductance vanishes as a power of the temperature. At low temperatures the term with  $n = 1$  will clearly dominate. For attractive interactions the perturbation theory breaks down in the zero-temperature limit, as could have been anticipated from the flow equation (3.10) in which  $t_1$  is a relevant perturbation for  $g > 1$ . At finite frequency and  $T = 0$ , we may derive a similar expression,

$$G(\omega) = \sum_{n=1}^{\infty} b_n \omega t_n^2 \omega^{2(n^2/g-1)}. \quad (3.12b)$$

Finally, we can evaluate the dc current-voltage characteristics at  $T = 0$  perturbatively in the hopping strength:

$$I(V) = \sum_{n=1}^{\infty} b_n V t_n^2 V^{2n^2/g-1}. \quad (3.12c)$$

While the coefficients  $b_n$  in (3.12) above are nonuniversal and depend on the high-frequency cutoff, their ratios are universal. They are tabulated in the Appendix. In a 1D wire of finite length  $L$ , the expressions (3.12) will be valid only on temperature, frequency, or voltage scales larger than  $T_L$ .

The above result that for repulsive interactions the conductance is zero at zero temperature can be traced to the fact that the tunneling density of states vanishes at zero energy in a Luttinger liquid. Specifically, the density of states for tunneling into the end of a semi-infinite Luttinger liquid is

$$\rho_{\text{end}}(\epsilon) \approx \epsilon^{1/g-1}. \quad (3.13)$$

Given this tunneling density of states, the conductance may be deduced from a simple argument based on Fermi’s ‘‘golden rule.’’ For instance, (3.12c) follows from the expression  $I \approx t^2 \int_0^V d\epsilon \rho_{\text{end}}(\epsilon) \rho_{\text{end}}(V - \epsilon)$  for the tunneling current. It should be emphasized that  $\rho_{\text{end}}(\epsilon)$  has a different energy dependence than the tunneling density of states into the middle of an infinite Luttinger liquid, which vanishes as  $\rho(\epsilon) \approx \epsilon^{(g+1/g)/2-1}$ . Although these are both constant for noninteracting electrons,  $g = 1$ , with interactions they will be general be different.

Similar power-law behavior of the conductance and  $I$ - $V$  characteristics has been found in studies of the effects of a series resistance on the single-junction Coulomb blockade.<sup>28,29</sup> In this case, the Caldeira-Leggett oscillators, which are used to phenomenologically model the series resistance, play a role analogous to the modes of the Luttinger liquid. In contrast, however, these models predict Ohmic resistance when the series resistance is zero. We predict Ohmic resistance when the series resistance of the one-dimensional leads is  $e^2/h$ .

### C. Phase diagram

Upon combining, the results for the scattering from a single barrier in the limit of a small barrier, from Sec. III A, and the limit of large barrier, or weak link, from Sec. III B, enables us to construct the full phase diagram. To be explicit, we consider a tight-binding model with nearest-neighbor hopping of electrons, in which one hopping matrix element (the ‘‘weak link’’) is reduced by a



fraction  $t$  with respect to all the other hopping strengths. When  $t$  is very close to one, it will induce some  $2k_F$  backscattering with strength,  $v_1 \approx 1-t$ . As we saw in Sec. III B, in the limit of small backscattering the  $2k_F$  contribution was a relevant perturbation for repulsively interacting electrons,  $g < 1$ . As one scales to lower energies or temperatures, the backscattering grows and scales out of the small-barrier perturbative regime. In Sec. III B, though, we saw that for repulsively interacting electrons, in the strong-barrier limit (small  $t$ ), the hopping strength scaled to zero at low energies and the link was insulating at zero temperature. It seems extremely plausible that one can join together these two perturbatively accessible regimes to argue that, regardless of how small the barrier is, at zero temperature it will cause total reflection and the link will be insulating. Indeed, as will be shown in Sec. VIII, for a special value of the interaction strength corresponding to  $g (= \frac{1}{2})$  an exact solution is possible. This solution indeed confirms that the smallest of barriers causes total reflection at  $T=0$ . This gives us confidence in concluding that, more generally, for repulsively interacting electrons a single barrier causes total reflection regardless of its strength. This is shown in the left of the phase diagram in Fig. 1.

For attractive interactions,  $g > 1$ , small  $2k_F$  backscattering was shown to be irrelevant in Sec. III A, whereas an initially small hopping across a weak link was shown to increase under renormalization. Once again, upon patching together these two perturbative limits we conclude that for attractive interactions the spinless electron gas behaves like a superfluid and at  $T=0$  suffers no reflection from even the largest of barriers. This is shown in the right side of Fig. 1.

Noninteracting electrons are, of course, marginal, and the degree of backscattering depends on the precise strength of the scattering potential. Why is this the case? Is it an accident, or is there a deeper physical reason underlying the fact that noninteracting electrons are on the border between two such different types of behavior? As

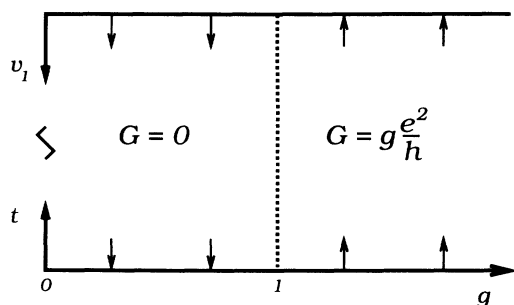


FIG. 1. The phase diagram for a one-channel gas of spinless interacting electrons incident upon a single barrier. Here  $g$  is the dimensionless conductance of the gas in the absence of the barrier, and  $G$  is the conductance in the presence of the barrier. The small arrows indicate the renormalization-group flows. Notice that for repulsive interactions ( $g < 1$ ) a single barrier is completely reflecting. The dashed line at  $g=1$ , which corresponds to a noninteracting electron gas, indicates a fixed line along which the conductance through the barrier varies continuously.

we discuss briefly below, this behavior can be attributed to the wave-particle duality of quantum mechanics. Indeed, near a weak link or barrier, there are two discrete, yet competing, processes taking place, one wave-like and the other particlelike. The discrete wavelike process is a  $2\pi$  slip in the phase difference  $\phi$  across the weak link, and the discrete particlelike process is that of hopping a single electron across the link. As is apparent from the phase diagram in Fig. 1, for repulsive interactions, with  $g < 1$ , the phase slips dominate, no electrons are transferred, and the link is insulating. For attractive interactions, the opposite occurs, with electrons being transferred but no voltage-generating phase slippage. For the Fermi liquid of noninteracting electrons both processes apparently coexist.

This can be understood with the following simple argument. Imagine slipping the phase across the weak link by  $2\pi$  but not allowing any electrons to hop across. Since the phase slippage causes a voltage glitch, we expect some charge to be transferred to the region of the weak link from the leads. Call this charge  $Q_{2\pi}$ . We can estimate  $Q_{2\pi}$  by combining Josephson's relation, which tells us that the time rate of change of the phase causes a voltage,  $V = \hbar \partial_t \phi / e$ , with the fact that the leads have a conductance given by  $G = ge^2/h$ . We write

$$Q_{2\pi} = \int dt I = G \int dt V(t), \quad (3.14)$$

and upon inserting Josephson's relation and integrating through one  $2\pi$  phase slip we find

$$Q_{2\pi} = ge. \quad (3.15)$$

We thus see that for repulsive interactions, when  $g < 1$ , the charge pulled in from the leads is *less than* the electron charge. Since this is not enough charge for a single electron hopping process, the charge cannot cross the weak link and the barrier is insulating. For attractive interactions,  $Q_{2\pi}$  is larger than  $e$ , and an electron can hop across the junction with some to spare, so one expects the link to be conducting. For a noninteracting Fermi liquid, precisely one electron of charge is transferred from the leads to the region of the weak link, and apparently sometimes it is transferred and sometimes it is not, leading to a conductance which depends on the barrier height.

While at best "hand waving" and at worst merely suggestive, it is nevertheless reassuring that such a simple argument can correctly reproduce the boundary between insulating and conducting behavior at  $g=1$ , as was shown via detailed calculations in earlier sections.

#### IV. TRANSMISSION OF SPINLESS ELECTRONS THROUGH A DOUBLE BARRIER AND RESONANT TUNNELING

In this section we consider the scattering of a spinless interacting electron gas incident upon a double-barrier potential. For noninteracting electrons, as the incident energy or wave vector of the electron is varied, Schrödinger's equation typically gives resonances, or peaks in the transmission. For a symmetric double-

barrier structure, the transmission at the peaks of these resonances is perfect, and the conductance is  $G^* = e^2/h$ . The width of the resonance is, of course, finite, even at  $T=0$ , and is determined by the height and width of the two barriers and the density of states of the electrons in the leads. Do such resonances survive in the presence of repulsive interactions when a Luttinger liquid is incident upon a double-barrier structure? Since even a single barrier causes total backscattering for repulsively interacting electrons, one might have been inclined to guess that a series arrangement of two barriers could only further enhance the backscattering, so that resonant transmission would be absent. In this section we show this is not the case. Rather, resonances are possible, but, in striking contrast to that for noninteracting electrons, they become infinitely sharp in the zero-temperature limit. As in Sec. III, we can analyze the backscattering from two barriers perturbatively in two limits, very weak and very large barriers, which we discuss below in Secs. IV A and IV B, respectively.

#### A. Weak barriers

Consider a double-barrier scattering potential  $V(x)$ , which is nonzero only within a distance  $d$  of the origin, and even there is much smaller than the Fermi energy. For noninteracting electrons the Born approximation can be used in this limit. At energies less than  $\hbar v_F/d$ , backscattering is simply proportional to the Fourier transform of  $V(x)$  at momenta  $2k_F$ :  $v_1 = \hat{V}(2k_F)$ . The condition for perfect resonant transmission is then simply that  $v_1 = 0$ . For a symmetric double-barrier potential, satisfying  $V(x) = V(-x)$ , the Fourier transform (and hence  $v_1$ ) is real, so that the resonance can typically be reached by tuning only one parameter, e.g., the incident electron energy. For an asymmetric potential, two parameters must be tuned to achieve a “true” resonance, by which we mean a resonance which has *perfect* transmission. As we shall see below, it is only such “true” resonances which can survive in the presence of repulsive electron interactions.

When electron interactions are present, the criterion for resonance in the weak-scattering limit is the same as for noninteracting electrons, namely a vanishing of  $\hat{V}(2k_F)$ . This follows readily from the perturbative analysis undertaken in Sec. III A. As can be seen from the RG flow equations in (3.4), the  $2k_F$  backscattering is always relevant for repulsive interactions. In its absence, though, the next most relevant term, namely  $4k_F$  backscattering, can be irrelevant. Specifically, provided  $g > \frac{1}{4}$ , the  $4k_F$  backscattering, which consists of two electrons being backscattered across the Fermi sea, and all higher-order processes, flow to zero at low energies. This implies that on resonance, when  $\hat{V}(2k_F)$  is zero, perfect transmission is expected. Indeed, the fact that the  $T=0$  on-resonance conductance will be  $G^* = ge^2/h$  follows directly from the perturbative calculation (3.5a).

On the other hand, for  $g < \frac{1}{4}$ , the  $4k_F$  backscattering grows at low energies, which suggests that the resonance will be destroyed in this case, as indeed we confirm in the next section. We mention in passing, though, that

“higher order” resonances are in principle possible. If, for example, both the  $2k_F$  and the  $4k_F$  backscattering could be *simultaneously* tuned to zero then, as (3.4a) shows, the resonance would survive all the way down to  $g = \frac{1}{9}$ . For  $g$  less than  $\frac{1}{9}$ , the  $6k_F$  backscattering becomes relevant and causes backscattering. In practice, however, we expect that all but the leading-order resonance will be extremely hard to “find,” so we focus below on that case only.

#### B. Resonant tunneling in the large-barrier limit

In this section we study resonant tunneling starting from the opposite limit, in which the tunneling barriers are very strong. In this limit, we anticipate that the physics associated with the Coulomb blockade<sup>11,12</sup> should become operative. Specifically, provided the capacitance associated with the “island” between the two barriers is small, the charge on the island will be fixed, and there will be a large-energy barrier to add another electron (namely the “charging energy,” roughly  $e^2/C$ ). Transmission through the island will thereby be strongly suppressed. However, if the chemical potential of the island is adjusted (i.e., by tuning a gate voltage) to the point where the energy cost to add another electron vanishes, we expect the possibility of a resonant transmission through the island.

In order to analyze this regime, and to see how it is related to the small-barrier limit in Sec. IV A, it is useful to consider a concrete model which consists of a perfect wire with two  $\delta$ -function barriers at positions  $x=0$  and  $d$ . In addition, we include a gate voltage  $V_G$ , which couples to the electrons between the barriers. As described in Sec. III A, the appropriate effective action in the  $\theta$  representation may be easily obtained:

$$S = S_0 + \int d\tau V \{ \cos[2\sqrt{\pi}\theta_1(\tau)] + \cos[2\sqrt{\pi}\theta_2(\tau) + k_F d] \} + V_G \frac{\theta_2(\tau) - \theta_1(\tau)}{\sqrt{\pi}}, \quad (4.1)$$

where  $\theta_1(\tau) = \theta(x=0, \tau)$ ,  $\theta_2(\tau) = \theta(x=d, \tau)$ , and  $S_0$  is the quadratic action (2.4a) which describes the pure Luttinger liquid. Here  $V$  is the strength of the two  $\delta$ -function potentials. It is again useful to integrate out the quadratic degrees of freedom away from the barriers, which enables the effective action to be expressed at low frequencies as

$$S_{\text{eff}} = \frac{1}{g} \sum_{i\omega_n} |\omega_n| \left[ |\theta(\omega_n)|^2 + \frac{\pi}{4} |n(\omega_n)|^2 \right] + \int d\tau V_{\text{eff}}(\theta(\tau), n(\tau)), \quad (4.2a)$$

where  $\theta = (\theta_1 + \theta_2)/2$ ,  $n = (\theta_2 - \theta_1)/\sqrt{\pi} + k_F d/2\pi$ , and

$$V_{\text{eff}}(\theta, n) = \frac{1}{2} U (n - n_0)^2 + V \cos 2\sqrt{\pi}\theta \cos \pi n. \quad (4.2b)$$

Here  $n$  can be interpreted as the number of particles between the two barriers, whereas  $\theta/\sqrt{\pi}$  is the number of particles which have been transferred across the two barriers, from one side to the other. Thus  $\theta$  plays a role similar to the  $\theta$  field entering in the single-barrier prob-

lem, (3.2) and (3.3). The “mass”  $U$ , which suppresses fluctuations in the particle number on the “island,” is equal to  $\hbar v_F/gd$ . Equation (4.2) is valid for frequencies smaller than  $U/\hbar$ . At higher frequencies, the effective action simply becomes that of two independent single barriers. The parameter  $n_0$ , which specifies the optimal value for  $n$ , is determined by the gate voltage and is equal to  $k_F d/2\pi + V_G/U$ . In general,  $n_0$  is a noninteger.

It is instructive to classify the symmetries of this model. The effective potential  $V_{\text{eff}}$  is invariant under the transformation  $\theta \rightarrow \theta + \sqrt{\pi}$ , as in the case of the single barrier. This transformation corresponds to the transfer of an electron from the left to the right leads. However, in the special case when  $n_0$  is tuned to be precisely a half-integer, there is an additional symmetry present:  $\theta \rightarrow \theta + \sqrt{\pi}/2$  and  $n \rightarrow 2n_0 - n$ . Roughly speaking, this symmetry corresponds to transferring an electron “half-way” across the double-barrier structure, in conjunction with a change in the charge state of the island. As we shall argue below, the presence of this extra symmetry when  $n_0 = \frac{1}{2}$  corresponds precisely to the condition for resonance.

In the limit of weak barriers,  $V \ll U$ , the action (4.2) is minimized when  $n = n_0$ , and we may safely integrate out  $n$ . We thereby arrive at a model in terms of  $\theta$  alone, which is similar to the single-barrier model studied in Sec. III A, except with

$$V_{\text{eff}}(\theta) = V \cos \pi n_0 \cos 2\sqrt{\pi} \theta + \frac{V^2}{2U} (\pi \sin \pi n_0 \cos 2\sqrt{\pi} \theta)^2 + \dots \quad (4.3)$$

It is thus clear that in the weak-barrier limit, the extra symmetry present when  $n_0$  is a half-integer corresponds to the vanishing of the  $2k_F$  backscattering term:  $v_1 \cos 2\sqrt{\pi} \theta$ . This was precisely the condition for resonance in the small-barrier limit, as established in Sec. IV A above.

On the other hand, when the barriers are very strong,  $V \gg U$ , the action will have deep minima when  $n$  is an integer [from the second term in (4.2b)], so that the discreteness of the electron charge is important. The degeneracy between these minima, however, is broken by the first term, proportional to  $U$ , so that a particular charge state of the “island” is preferred, with an energy gap of order  $U$  to other charge states. This is precisely the physics of the Coulomb blockade, in which transmission across the island is impeded by an energy barrier resulting from a small capacitance of the island. In this case,  $U$  plays the role of the single electron charging energy  $e^2/C$ . When  $n_0$  is tuned to be a half-integer, we have the additional symmetry discussed above, and two charge states become degenerate. This corresponds to the situation when the chemical potential of the island is adjusted so that the energy cost to add another electron to the island vanishes. In Fig. 2(a) we display the positions of the minima in the action as a function of  $\theta$  and  $n$ .

In the large-barrier limit, the partition function on resonance will be dominated by instantons (or tunneling events) connecting these degenerate minima. These correspond physically to hopping events in which electrons

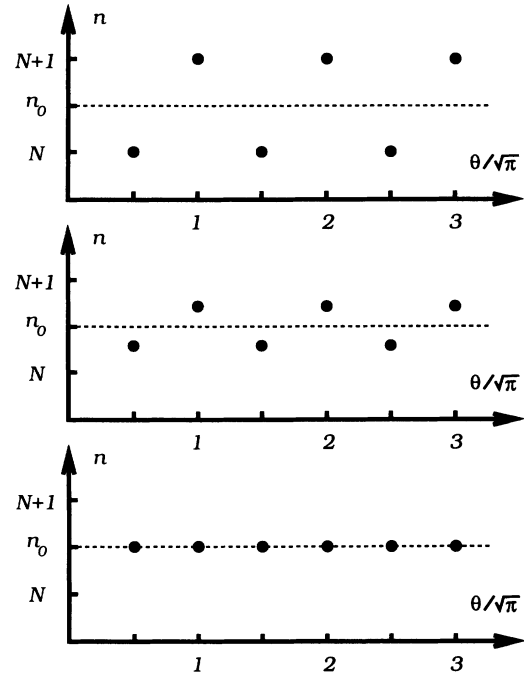


FIG. 2. Positions of the minima of the function  $V_{\text{eff}}(\theta, n)$  [defined in Eq. (4.2b)] in the  $\theta$ - $n$  plane: (a) for  $K=1$ , (b) for intermediate values of  $K$ , and (c) for  $K=0$ . Here  $\theta/\sqrt{\pi}$  is the number of (spinless) electrons transferred across the double-barrier structure, and  $n$  is the number of particles between the two barriers. Notice that in (c) there is an effective symmetry under transferring half of an electron across the double-barrier structure.

hop onto or off of the island. The island may thus effectively be described as a two-level system, in which hopping on and off the island corresponds to switching back and forth between the two levels. This situation is most easily analyzed using the “Coulomb-gas” representation, which may be viewed either as an expansion of the partition function in the  $\theta$  representation in terms of instantons or equivalently as an expansion in the  $\phi$  representation (as in 3.11) in powers of the hopping matrix elements, connecting the island and the left and right leads,  $t_+$  and  $t_-$ . The boson fields will mediate an effective interaction between these “charges.” In contrast to the single-barrier case in (3.11), though, we now have four kinds of charges: hops to either the left or to the right across either of the two barriers ( $t_+$  and  $t_-$  representing the “charge” fugacities). Care must be taken in treating the two-level nature of the island. Specifically, the ordering of the hops is constrained by the fact that the charge state on the island can only change by 1, which means that hops onto and off the island must alternate in time. If  $q_i = \Delta\theta/\sqrt{\pi} = \pm 1/2$  denotes the charge transferred to the right in a hopping event and  $r_i = \Delta n/2 = (-1)^i/2$  denotes the change in the charge on the island, then the partition function in the “Coulomb-gas” representation may be written for the symmetric barrier case,

$t_+ = t_- = t$ , as

$$Z = \sum_n \sum_{q_i} t^{2n} \int_0^\beta d\tau_{2n} \cdots \int_0^{\tau_2} d\tau_1 \exp \left[ \sum_{i < j} V_{ij} \right], \quad (4.4)$$

$$V_{ij} = \frac{2}{g} (q_i q_j + K r_i r_j) \ln(\tau_i - \tau_j) / \tau_c.$$

As in (3.11),  $\tau_c \approx E_F^{-1}$  is a short-time cutoff. The more general case of an asymmetric barrier,  $t_+ \neq t_-$ , is considered in Appendix B. The initial value of  $K$  is 1; however, as we shall see, its value flows in the renormalization group. The dimensionless lead conductance  $g$ , on the other hand, is not renormalized. (This is related to the fact that the sign of the charges  $r_i$  must alternate in time, whereas the charges  $q_i$  can have any ordering). We analyze the above model using the real-space perturbative renormalization-group method invented by Anderson, Yuval, and Hamann.<sup>24</sup> Some details of this calculation are presented in Appendix B. To leading (nonvanishing) order in  $t$  the resulting RG flow equations are

$$dK/dl = -8\tau_c^2 t^2 K, \quad (4.5a)$$

$$dt/dl = t [1 - (1+K)/4g]. \quad (4.5b)$$

In order to interpret (4.5) it is useful to consider intermediate values of  $V/U$  in (4.2). As this ratio is reduced from large values, the value of  $n$  at the minima deviates from an integer, as shown in Fig. 2(b). This is a consequence of the fact that the electrons on the island can now virtually tunnel into the leads, so that the average charge on the island is reduced. Therefore, during a tunneling event between these minima,  $n$  changes by an amount less than 1, and the corresponding Coulomb-gas model is like (4.3), except with  $K$  less than 1. But notice that under the renormalization group (4.5a),  $K$  flows to smaller values, which corresponds to smaller values of  $V/U$ . If  $K$  ultimately flows to zero, then we arrive at the situation in Fig. 2(c), in which the discrete charge of the island, which is characterized by  $n$ , no longer plays any role. In this limit ( $K=0$ ) the Coulomb-gas model (4.4) becomes identical to that describing a single barrier (3.11), except that now we have the additional ‘‘resonance symmetry’’ under  $\theta \rightarrow \theta + \sqrt{\pi}/2$ . A single charge  $q_i$  therefore corresponds to the transfer of ‘‘half’’ an electron across the structure. The presence of the double-barrier structure on resonance allows electrons to be transferred across the junction in two steps. The hopping of an electron onto the island is therefore like transferring an electron ‘‘half-way’’ across the junction, or equivalently, transferring ‘‘half’’ an electron across the junction.

### C. On-resonance phase diagrams

In this section we analyze the flow equations derived in the preceding sections for resonant tunneling of spinless interacting electrons and unify them into a single set of phase diagrams. The results are summarized in the phase diagram displayed in Fig. 3, which corresponds to spinless electrons incident on a symmetric double-barrier structure precisely on resonance. In the weak-barrier

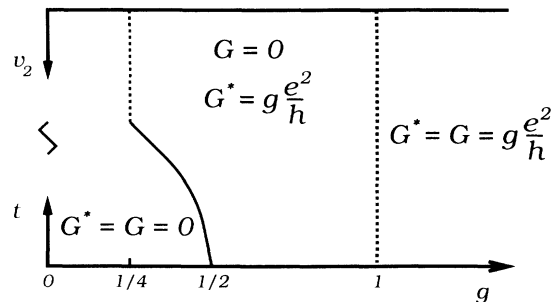


FIG. 3. On-resonance phase diagram for spinless interacting electrons incident upon a double-barrier structure. The conductance off resonance is denoted by  $G$ , whereas the conductance on resonance is denoted by  $G^*$ . The dashed line at  $g=1$  is the fixed line for transmission off resonance, corresponding to noninteracting electrons, while the dashed line at  $g=1/4$  is the fixed line for transmission on resonance. The solid line between  $g=1/4$  and  $1/2$  is a line of Kosterlitz-Thouless separatrices.

limit, shown in the upper part of Fig. 3, when the resonance condition  $v_1 \equiv V(2k_F) = 0$  is satisfied, we saw in Sec. IV A that all other perturbations are irrelevant provided  $g > 1/4$ . In this case perfect transmission was found on resonance. For  $g < 1/4$ , however, the  $4k_F$  backscattering term  $v_2$  is relevant and grows as one scales to lower energies. For  $g = 1/4$ , the  $v_2$  perturbation is marginal, and a ‘‘fixed line,’’ with a conductance on resonance that varies continuously, is expected. This is directly analogous to the fixed line in the single-barrier phase diagram at  $g=1$  (Fig. 1), which corresponds to noninteracting electrons being partially backscattered by the marginal  $2k_F$  backscattering term.

In the large-barrier or small-tunneling limit, considered in Sec. IV B, the RG flows for a symmetric double barrier are given by (4.5). For  $g > 1/2$  it is clear that an initially small hopping  $t$  grows under the RG transformation, since  $K$  is always less than 1 (and positive). It seems extremely likely that the RG flows in this case join on to the flows on resonance in the small-backscattering limit, so that perfect transmission follows. It is worth emphasizing that this is entirely consistent with what happens on resonance for noninteracting electrons, where perfect transmission is found regardless of the strength of the (symmetric) double-barrier potential. For  $g < 1/4$ , on the other hand, it is clear from (4.5) that the hopping strength  $t$  flows to zero, and the resonant tunneling is destroyed completely at zero temperature. This matches nicely the analysis in the small-backscattering limit, where we found a growing  $4k_F$  backscattering term in this case.

For  $1/4 < g < 1/2$ , although a small hopping  $t$  will flow to zero, as  $t$  is increased a separatrix is crossed (at  $t^*$ ) above which the RG flows are to large  $t$ . As shown in Fig. 4, this separatrix flows into a Kosterlitz-Thouless fixed point,<sup>25</sup> described by (4.5), at  $K_c = 4g - 1$  and  $t = 0$ . Thus, as  $t$  is decreased through  $t^*$ , the resonance at  $T = 0$  will disappear at a sharp Kosterlitz-Thouless phase transition. For  $g = 1/4$ , the system flows into a fixed line with

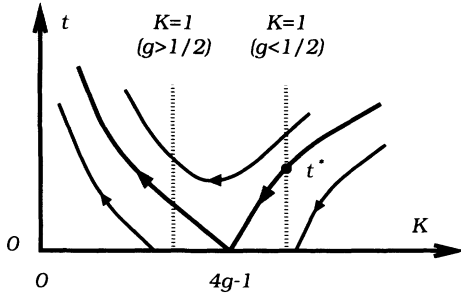


FIG. 4. Schematic renormalization-group flows for resonant tunneling when  $g > \frac{1}{4}$ , as obtained from the flow equations (4.5a). When  $g < \frac{1}{2}$  there is a Kosterlitz-Thouless separatrix which is crossed as the hopping strength between the leads and the island,  $t$ , is increased through  $t^*$ . For  $g > \frac{1}{2}$ , the renormalization-group flow begins to the left of the Kosterlitz-Thouless fixed point, and always flows to strong coupling. This corresponds to resonant transmission.

$K_c = 0$ , along which the renormalized value of  $t$  varies continuously. If the bare  $t$  is just slightly greater than  $t^*$ , the flows are into the perturbatively accessible regime, and the conductance can be shown to vary as  $G \propto (t - t^*)^2$ . As  $t$  is increased further, the conductance on this fixed line continues to increase. It is reassuring that for  $g = \frac{1}{4}$  we have thus been able to access both ends of the fixed line, at small and large barriers. This fixed line is shown as a dashed line in Fig. 3. By generalizing the simple physical argument in Sec. III C to allow for tunneling “half an electron” across the junction, it is easy to understand why the fixed line for this process occurs at  $g = \frac{1}{4}$ .

It is instructive to briefly discuss the effects of an asymmetric double-barrier structure. For noninteracting electrons, the transmission through a large but asymmetric double-barrier structure takes the form

$$T = \frac{2t_+ t_-}{t_+^2 + t_-^2}, \quad (4.6)$$

where  $t_{\pm}$  is the transmission through the right and left barriers, respectively. It is clear from (4.6) that an asymmetric barrier may exhibit appreciable, but not perfect, transmission. In the limit of small barriers this is also clear, since for an asymmetric barrier, upon tuning a single parameter (such as the electron energy) in general the real and imaginary parts of the  $2k_F$  backscattering will not simultaneously vanish. By this reasoning, we expect that in the presence of repulsive interactions (where  $2k_F$  backscattering is relevant) the resonance will be completely destroyed at  $T = 0$  by an asymmetry. It is instructive to see how this occurs in the large-barrier limit. In Appendix B we derive the general flow equations for an asymmetric barrier, working perturbatively in the strength of the hopping  $t$  [see Eq. (B4)]. In Figs. 5(a)–5(c), we sketch schematic renormalization-group flows obtained from these, projected into the  $t_+ t_-$  plane for various values of  $g$ . In each figure, the limit of  $t_+ \rightarrow \infty$  or  $t_- \rightarrow \infty$  corresponds to an absence of one of the two bar-

riers. Thus, the upper right corner of each figure corresponds to the perfect conductor with no barriers. The top and right axes, in which either  $t_+$  or  $t_-$  is infinite, correspond to a *single barrier*.

For attractive interactions,  $g > 1$  [Fig. 5(a)], we have perfect transmission even off resonance, and all flows lead to the perfectly conducting fixed point in the upper right corner. For  $g = 1$  [Fig. 5(b)], a single barrier is a marginal perturbation, so the top and right axes are fixed lines, denoted by the dashed lines in Fig. 5(b). However, a symmetric barrier has perfect resonant transmission, so that on the diagonal the flows are into the perfectly transmitting fixed point. This is consistent with the physics con-

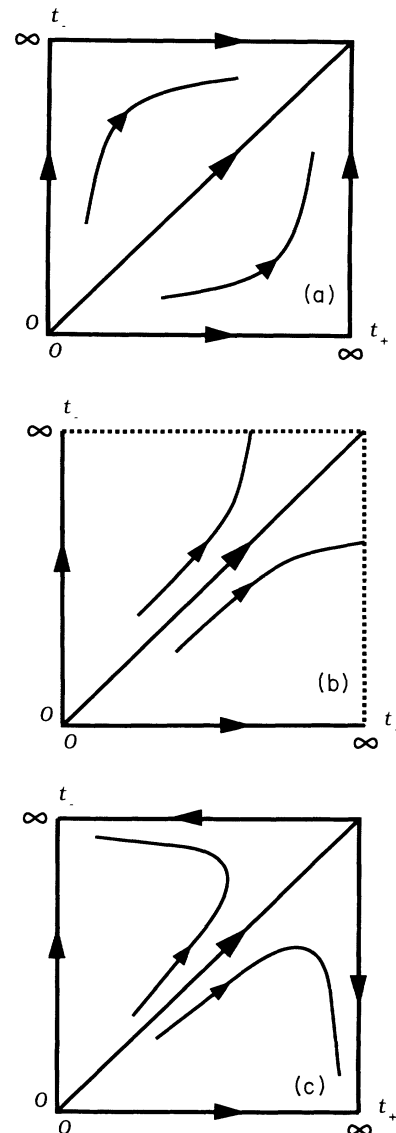


FIG. 5. Schematic renormalization-group flows for a spinless electron gas incident upon two inequivalent barriers, with hopping strengths  $t_+$  and  $t_-$  to the left and right leads, as obtained from the flow equations in Appendix B for (a)  $g > 1$ , corresponding to attractive interactions, (b)  $g = 1$ , noninteracting electrons, and (c)  $\frac{1}{2} < g < 1$ , repulsive interactions. The dashed line in (b) indicates a fixed line.

tained in Eq. (4.6), since a slightly asymmetric barrier is seen to exhibit almost perfect transmission for noninteracting electrons. For repulsive interactions and  $\frac{1}{2} < g < 1$  [Fig. 5(c)], a single barrier is insulating. Therefore, the top and right axes flow to the fixed point with a single infinite high barrier. Though a symmetric barrier flows along the diagonal to the perfect conductor, an asymmetric barrier ultimately flows to one of the two insulating fixed points. Notice that although the barriers may initially get smaller under renormalization, the larger of the two barriers eventually turns around and grows. Finite temperature, of course, can cut off the renormalization-group flows, and, as discussed in Sec. VII, a slightly asymmetric barrier can still exhibit large conductance when the temperature is not too low. For  $\frac{1}{4} < g < \frac{1}{2}$ , the Kosterlitz-Thouless transition is present, and the flow diagram becomes somewhat more complicated. In this case, a line of Kosterlitz-Thouless separatrices divides the flows from the infinite single-barrier fixed point and the infinite double-barrier fixed point. For  $g < \frac{1}{4}$  the system is always insulating.

## V. TRANSMISSION THROUGH A SINGLE BARRIER FOR ELECTRONS WITH SPIN

In this section we generalize the considerations of Sec. III to include electrons with a spin degree of freedom, and analyze transmission through a single barrier. We defer a discussion of resonances in the double-barrier case until Sec. VI. When there are no barriers, as we have seen in Sec. II, the Luttinger-liquid phase is characterized by a charge conductivity  $g_\rho$  and a spin “conductivity”  $g_\sigma$ . Moreover, in a model with SU(2) spin symmetry,  $g_\sigma = 2$ . In this section we will find it useful to consider arbitrary values of  $g_\rho$  and  $g_\sigma$ ; however, it must be kept in mind that when  $g_\sigma > 2$ , the Luttinger-liquid phase is unstable to formation of a spin gap.

Our approach follows closely that for the spinless case: We first study the effects of a very small barrier, in Sec. V A, and then analyze the opposite limit of a large barrier or weak tunneling in Sec. V B. For  $g_\sigma = 2$ , the case with spin symmetry, the results are very similar to the spinless case. Namely, for repulsive interactions,  $g_\rho < 2$ , an arbitrarily small barrier will cause total reflection and insulating behavior at zero temperature. Again, there are power-law corrections at finite temperatures with an exponent which is slightly modified from the spinless case. For attractive interactions, on the other hand, we find perfect transmission at  $T = 0$ .

More generally, when  $g_\sigma \neq 2$ , there is a richer class of possible behaviors, for there are now four possible phases, corresponding to either perfect transmission or perfect reflection of the charge and spin degrees of freedom. For any given value of the lead conductances  $g_\sigma$  and  $g_\rho$ , at least one of these four phases is found to be stable. However, in contrast to the spinless case, our perturbative analysis in the limits of small and large barriers indicates that for certain values of  $g_\sigma$  and  $g_\rho$ , there must be nontrivial phase transitions at an intermediate barrier height separating two of the phases. This was emphasized recently by Furusaki and Nagaosa.<sup>30</sup> By carefully tuning

the lead conductances  $g_\sigma$  and  $g_\rho$ , we are able to perturbatively access these nontrivial critical fixed points as described in Sec. V D. We find that right at the transition, both charge and spin are partially transmitted and partially reflected. But, most striking, the transmission coefficients are shown to be universal, depending only on the lead conductances.

### A. Small barriers

Consider first the limit of a small barrier. As before, we add a small scattering potential  $V(x)$ , which is nonzero only near the origin. It is again convenient to perform a partial trace over those quadratic degrees of freedom away from the origin, which enter into the Luttinger-liquid action (2.7). With spin, when  $V(x) = 0$ , the action in the  $\theta$  representation may be written

$$S_0 = \frac{1}{g_\rho} \sum_{i\omega_n} |\omega_n| |\theta_\rho(\omega_n)|^2 + \frac{1}{g_\sigma} \sum_{i\omega_n} |\omega_n| |\theta_\sigma(\omega_n)|^2. \quad (5.1)$$

The addition of a local perturbation will introduce additional terms to this action. These may be arrived at by translating the scattering term

$$\delta H = \int dx V(x) (\psi_\uparrow^\dagger \psi_\uparrow + \psi_\downarrow^\dagger \psi_\downarrow) \quad (5.2)$$

into the boson variables. Since the potential  $V(x)$  is assumed to be nonzero only near the origin, it is possible to perform a gradient expansion as in Sec. III A. A term will thus be generated of the form

$$\begin{aligned} \delta S &= v_e \int d\tau \frac{1}{2} (\cos 2\sqrt{\pi}\theta_\uparrow + \cos 2\sqrt{\pi}\theta_\downarrow) \\ &= v_e \int d\tau \cos\sqrt{\pi}\theta_\rho \cos\sqrt{\pi}\theta_\sigma, \end{aligned} \quad (5.3)$$

where  $v_e$  is the Fourier component  $V(2k_F)$  of  $V(x)$ , and the  $\theta$  fields are evaluated at  $x = 0$ . Here we have used (2.5) to relate  $\theta_\rho$  and  $\theta_\sigma$  to  $\theta_\uparrow$  and  $\theta_\downarrow$ .

In general, though, when considering possible perturbations about (5.1), we must consider *all* terms which are consistent with the symmetries of the problem, since they will all be generated under renormalization in any case. The important symmetry is that the action must remain under either of the transformations  $\theta_\uparrow \rightarrow \theta_\uparrow + \sqrt{\pi}$  or  $\theta_\downarrow \rightarrow \theta_\downarrow + \sqrt{\pi}$ , which correspond to moving all of the spin-up (or -down) particles over by one interelectron spacing. Equivalently, the action must be invariant under the combined transformations  $\theta_\rho \rightarrow \theta_\rho + \sqrt{\pi}$  and  $\theta_\sigma \rightarrow \theta_\sigma + \sqrt{\pi}$ . Thus, if we ignore terms involving spatial derivatives (which are less relevant), the most general perturbation to the Lagrangian can be expressed as a function  $V_{\text{eff}}(\theta_\sigma, \theta_\rho)$ , which is periodic in both arguments with period  $\sqrt{\pi}$ . We can thus write

$$\delta S = \int d\tau V_{\text{eff}}(\theta_\sigma(\tau), \theta_\rho(\tau)), \quad (5.4a)$$

where

$$V_{\text{eff}}(\theta_\sigma, \theta_\rho) = \sum'_{n_\sigma, n_\rho} \frac{1}{4} v(n_\sigma, n_\rho) e^{i\sqrt{\pi}(n_\rho \theta_\rho + n_\sigma \theta_\sigma)}. \quad (5.4b)$$

The  $\sum'$  indicates a sum over all integers  $n_\sigma, n_\rho$  such that  $n_\sigma + n_\rho$  is even. Since the original Hamiltonian is Hermi-

tion, the function  $V_{\text{eff}}$  must be real, so that the coefficients in (5.4) satisfy  $v(n_\sigma, n_\rho) = v(-n_\sigma, -n_\rho)^*$ . Moreover, due to spin-rotational invariance, one has  $v(n_\sigma, n_\rho) = v(-n_\sigma, n_\rho)$ . If the original potential  $V(x)$  was symmetric,  $V(x) = V(-x)$ , then the perturbation in (5.4) will also be invariant under  $\theta_\rho \rightarrow -\theta_\rho$ , which implies that  $v(n_\sigma, n_\rho) = v(n_\sigma, -n_\rho)$ , in which case all the  $v(n_\rho, n_\sigma)$  are real.

A renormalization-group analysis, perturbative in the  $v(n_\rho, n_\sigma)$ , can be carried out as in Sec. III A, and the leading-order flow equations are

$$dv(n_\rho, n_\sigma)/dl = \left[ 1 - \frac{n_\rho^2}{4} g_\rho - \frac{n_\sigma^2}{4} g_\sigma \right] v(n_\rho, n_\sigma). \quad (5.5)$$

For the case with SU(2) spin symmetry,  $g_\sigma = 2$ , the most relevant perturbation is  $v_e = v(n_\sigma = 1, n_\rho = 1)$ . This

corresponds physically to  $2k_F$  backscattering of the electrons. [For a symmetric potential  $v_e$  is real, and the contribution to the action from this backscattering is given explicitly in (5.3).] As in the spinless case, this is relevant for repulsive interactions,  $g_\rho < 2$ . For noninteracting interacting electrons  $g_\sigma = g_\rho = 2$  it is marginal. For attractive interactions  $g_\rho > 2$ , it is irrelevant; however, in this case it should be emphasized that there will in general be an instability towards a singlet superconducting phase, and the spin part of the action will no longer be massless.

Allowing for more general values of  $g_\sigma$ , we follow Furusaki and Nagaosa<sup>30</sup> and plot curves in the  $g_\rho - g_\sigma$  plane above and to the right of which the operator in question is irrelevant. For example, the  $2k_F$  backscattering  $v_e$  is irrelevant for values of  $g_\rho$  and  $g_\sigma$  above and to the right of the line  $g_\rho + g_\sigma = 4$ , as shown in Fig. 6(a). Other important operators include the process which backscatters both a spin-up and a spin-down electron,

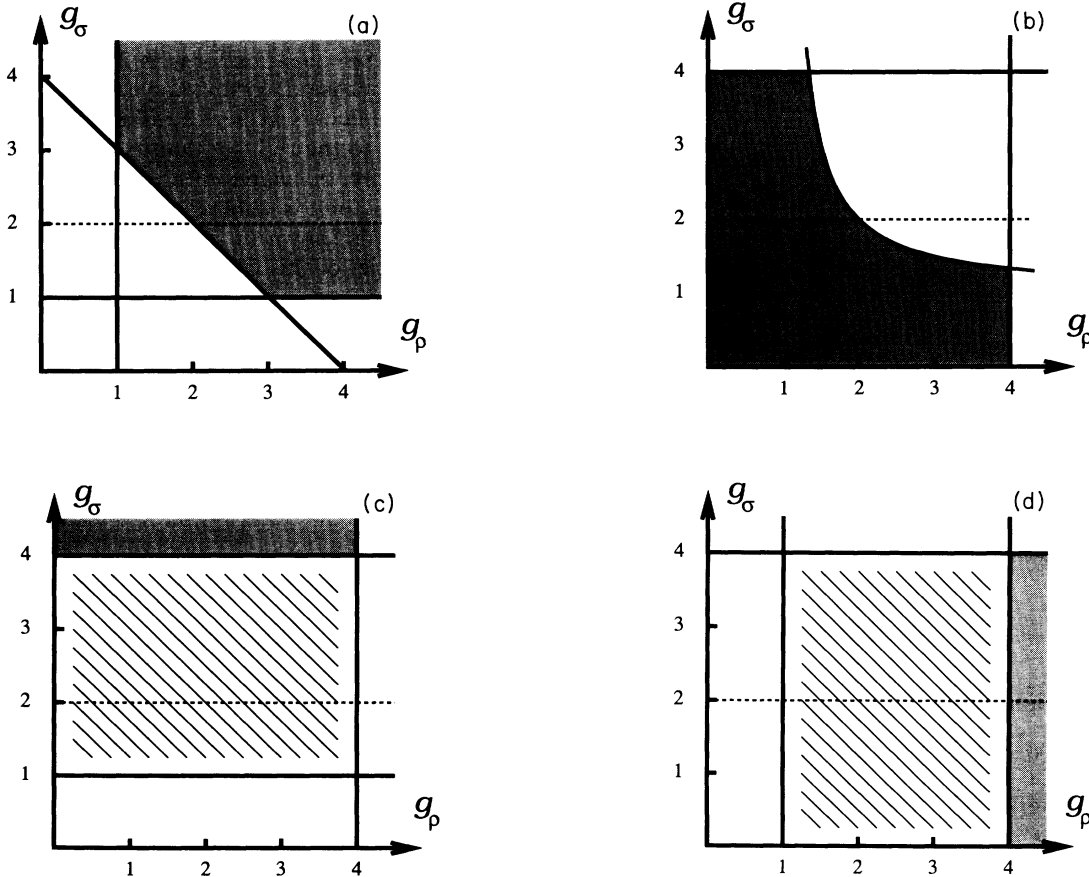


FIG. 6. Regions of stability of various phases of the interacting electron gas with spin, incident upon a single barrier, shown in the  $g_\rho - g_\sigma$  plane: (a) The shaded region corresponds to the phase in which both spin and charge are perfectly transmitted, and was obtained in the limit of weak backscattering, Eq. (5.5). (b) Shaded region corresponds to the phase in which both charge and spin are completely reflected, obtained in the limit of large barriers from Eq. (5.10). (c) Shaded region corresponds to the phase which is a spin conductor and/or charge insulator, as discussed in Sec. V C. (d) Shaded region is a phase which is a charge conductor and/or spin insulator. In (c) and (d) the cross-hatched regions indicate stability of the respective “mixed” phases in the case of a barrier with inversion symmetry. In each of the figures the dashed line at  $g_\sigma = 2$  corresponds to a spinful electron gas with SU(2) spin symmetry.



which takes the form

$$\delta S_\rho = \int d\tau \frac{1}{2} (v_\rho e^{i2\sqrt{\pi}\theta_\rho} + \text{c.c.}), \quad (5.6a)$$

where the coefficient  $v_\rho = \frac{1}{2}v(n_\sigma=0, n_\rho=2)$ . The analogous operator for the spin degrees of freedom,

$$\delta S_\sigma = \int d\tau \frac{1}{2} (v_\sigma e^{i2\sqrt{\pi}\theta_\sigma} + \text{c.c.}), \quad (5.6b)$$

with  $v_\sigma = \frac{1}{2}v(n_\sigma=2, n_\rho=0)$ , corresponds physically to a backscattering of an up-spin electron and a down-spin electron which are incident from opposite directions, so that the net charge momentum is unchanged. The operator  $v_\rho$  is irrelevant to the right of the line  $g_\rho=1$ , and  $v_\sigma$  is irrelevant above the line  $g_\sigma=1$ , as shown in Fig. 6(a). Below or to the left of these lines, the operators are relevant, and initially weak scattering grows under renormalization to lower energies. The fate of the physics in this regime will be analyzed in Secs. V B and V C below.

As for the spinless electron gas, the conductance can be calculated straightforwardly as a perturbation expansion in powers of the coefficients  $v(n_\sigma, n_\rho)$  in (5.4),

$$G(T) = e^2/h \left[ g_\rho - \sum_{n_\sigma, n_\rho} ' c_T(n_\sigma, n_\rho) |v(n_\sigma, n_\rho)|^2 \times T^{(n_\sigma^2 g_\sigma + n_\rho^2 g_\rho)/2 - 2} \right].$$

Similar expressions may be derived for  $G(\omega)$  and  $I(V)$ , and the coefficients  $c_T$ ,  $c_\omega$ , and  $c_V$  are tabulated in Appendix A.

### B. Large-barrier limit

Consider now the transmission of a spin electron gas through a very large barrier. This limit can best be described by considering two semi-infinite Luttinger liquids coupled together by a weak hopping matrix element  $t$ . In this case, the effective action in terms of the phase differences across the junction  $\phi_{\rho, \sigma} = (\phi_{\rho, \sigma+} - \phi_{\rho, \sigma-})/2$  may be written

$$S_0 = g_\rho \sum_{i\omega_n} |\omega_n| |\phi_\rho(\omega_n)|^2 + g_\sigma \sum_{i\omega_n} |\omega_n| |\phi_\sigma(\omega_n)|^2. \quad (5.7)$$

To this we add a hopping term,

$$\delta H \approx -t_e [ \psi_{+\uparrow}^\dagger(x=0)\psi_{-\uparrow}(x=0) + \psi_{+\downarrow}^\dagger(x=0)\psi_{-\downarrow}(x=0) + \text{H.c.} ]. \quad (5.8a)$$

The bosonized form of this expression leads to

$$\begin{aligned} \delta S_1 &= \frac{1}{2} t_e \int d\tau (\cos 2\sqrt{\pi}\phi_\uparrow + \cos 2\sqrt{\pi}\phi_\downarrow) \\ &= t_e \cos 2\sqrt{\pi}\phi_\rho \cos 2\sqrt{\pi}\phi_\sigma. \end{aligned} \quad (5.8b)$$

In general, terms involving multiple hops will be generated under the renormalization group, so we should again consider all such terms consistent with the symmetries. The most general hopping term may be written as

$$\delta S = \sum_{n_\sigma, n_\rho} ' t(n_\sigma, n_\rho) \int d\tau \cos 2n_\rho \sqrt{\pi}\phi_\rho \cos 2n_\sigma \sqrt{\pi}\phi_\sigma, \quad (5.9)$$

where  $\sum'$  indicates a sum over non-negative integers  $n_\sigma$  and  $n_\rho$  such that  $n_\sigma + n_\rho$  is even. Note that by time-reversal invariance  $t(n_\sigma, n_\rho)$  is necessarily real. The single-electron hopping term is then  $t_e = t(n_\sigma=1, n_\rho=1)$ . Other important low-order terms are  $t_\rho \equiv t(n_\sigma=0, n_\rho=2)$ , which corresponds to hopping a singlet pair across the junction (two charges, but no spin) and  $t_\sigma \equiv t(n_\sigma=2, n_\rho=0)$ , which corresponds to flipping a pair of spins (a spin 1 is transferred, but no charge). The lowest-order renormalization-group flows for these perturbations are

$$dt(n_\sigma, n_\rho)/dl = \left[ 1 - \frac{n_\rho^2}{g_\rho} - \frac{n_\sigma^2}{g_\sigma} \right] t(n_\sigma, n_\rho). \quad (5.10)$$

For  $g_\sigma=2$ , the case with SU(2) spin symmetry, all hopping terms flow to zero for repulsive interactions  $g_\rho < 2$ ; however,  $t_e$  increases under the RG flows for  $g_\rho > 2$ . Once again, these results match nicely the analysis in the small- $V(x)$  limit, and we conclude that a single barrier causes complete reflection (i.e., insulating behavior) at  $T=0$ . The system is an insulator for repulsive interactions. The phase diagram for  $g_\sigma=2$  is similar to the spinless electron phase diagram shown in Fig. 1, except that the fixed line occurs at  $g_\rho=2$  rather than  $g=1$ , and the conductance to the right of that fixed line is  $G = g_\rho e^2/h$ . More generally, the values of  $g_\rho$  and  $g_\sigma$  for which the insulating fixed point is stable (i.e., all hopping parameters  $t$  flow to zero) is shown in the shaded region of Fig. 6(b). The boundaries of this region are determined by the most relevant hopping terms, which are  $t_e$ ,  $t_\rho$ , and  $t_\sigma$ .

In the regions in which the insulating fixed point is stable, the conductance at finite energies may again be computed perturbatively. We find at finite temperatures

$$G(T) = \sum_{n_\sigma, n_\rho} ' d_T(n_\sigma, n_\rho) t(n_\sigma, n_\rho)^2 T^{2(n_\rho^2/g_\rho + n_\sigma^2/g_\sigma - 2)}, \quad (5.11)$$

with similar expressions for  $G(\omega)$  and  $I(V)$ . The coefficients  $d_T$ ,  $d_\omega$ , and  $d_V$  are computed in the Appendix.

It is again illuminating to consider the Coulomb-gas representation of the partition function obtained by expanding  $Z$  in powers of  $t_e$ ,  $t_\rho$ , and  $t_\sigma$ . We may classify the different kinds of ‘‘charges’’ (or hops) by defining  $q_i = \pm n_\rho$  to be the charge transferred across the junction and  $s_i = \pm n_\sigma$  to be the spin transferred across the junction. Thus, for a  $t_e$  hop,  $q_i = \pm 1$  and  $s_i = \pm 1$ , whereas for a  $t_\rho$  hop,  $q_i = \pm 2$  and  $s_i = 0$ . As in the spinless case, integrating out the bosonic  $\phi$  fields in (5.7) will mediate a logarithmic interaction between these ‘‘charges’’ of the form

$$V_{ij} = \left[ \frac{2}{g_\rho} q_i q_j + \frac{2}{g_\sigma} s_i s_j \right] \ln(\tau_i - \tau_j) / \tau_c. \quad (5.12)$$

This Coulomb-gas model can also be understood in the  $\theta$  representation in the large-backscattering limit. In this case, the effective potential  $V_{\text{eff}}(\theta_\sigma, \theta_\rho)$  has deep minima, depicted in Fig. 7, which are related by the symmetry under  $\theta_\sigma \rightarrow \theta_\sigma \pm \sqrt{\pi}$  and  $\theta_\rho \rightarrow \theta_\rho \pm \sqrt{\pi}$ . The partition func-

tion is dominated by tunneling events, or instantons, between the nearby minima, as indicated in Fig. 7. These instantons correspond precisely to the hopping events  $t_e$ ,  $t_\rho$ , and  $t_\sigma$  described above, and the interactions between these instantons are described by (5.12).

### C. “Mixed” phases

We have seen that the conducting phase in which both spin and charge are perfectly transmitted (i.e., the conducting fixed point) is described by the limit in which  $V_{\text{eff}}(\theta_\sigma, \theta_\rho) = 0$ , and is stable when all the perturbations  $v(n_\sigma, n_\rho)$  in (5.4) are irrelevant. The phase in which both spin and charge are completely reflected (i.e., the insulating fixed point) is described by the limit in which  $V_{\text{eff}}(\theta_\sigma, \theta_\rho)$  is large, and is stable when the instantons (or hopping events) connecting the various minima are bound and hence irrelevant. A third possibility is to have the potential experienced by  $\theta_\sigma$  and  $\theta_\rho$  strongly anisotropic, so that motion is free along one direction, but is blocked by a very high barrier in the other direction. For example, when  $v_\rho = v(n_\sigma = 0, n_\rho = 2)$  in (5.4b) is large, there is a large barrier for transporting charge across the junction, but the spin may tunnel freely. This situation describes a charge insulator and/or spin conductor. Similarly, large  $v_\sigma = v(n_\sigma = 2, n_\rho = 0)$  describes a charge conductor and/or spin insulator. These “mixed” phases will be stable provided both the additional perturbations  $v(n_\sigma, n_\rho)$  are all irrelevant *and* the instantons connecting the different minima are bound.

For the case of the charge insulator and/or spin conductor with large  $v_\rho$ , the instantons (or hopping events) connecting adjacent minima in the  $\theta_\rho$  direction are equivalent to the  $t_\rho$  hops described in the preceding section. As (5.10) shows, they are irrelevant provided  $g_\rho < 4$ .

The most relevant possible perturbation about this “mixed” phase is  $2k_F$  backscattering of an electron:

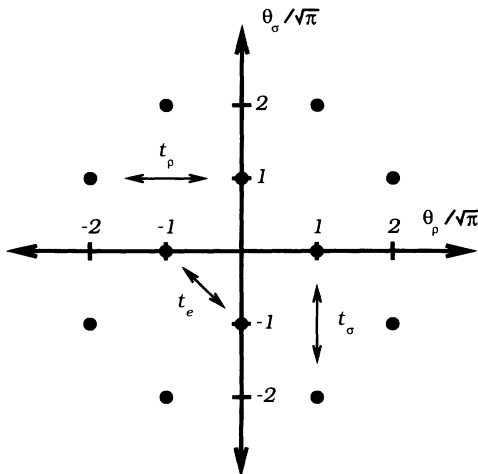


FIG. 7. Positions of the minima of the function  $V_{\text{eff}}(\theta_\sigma, \theta_\rho)$ , defined in (5.4b), in the  $\theta_\sigma$ - $\theta_\rho$  plane. Tunneling events between these minima are denoted by  $t_e$ ,  $t_\sigma$ , and  $t_\rho$  and correspond to transfer of charge and spin across the barrier, as described in detail in the text.

$v_e = v(n_\sigma = 1, n_\rho = 1)$ . To determine its effect, we write the effective action [assuming SU(2) spin symmetry] from (5.1) and (5.4) in terms of  $v_\rho$  and  $v_e$  as

$$S = S_0 = \int d\tau \mathcal{R}(v_\rho e^{i2\sqrt{\pi}\theta_\rho} + v_e e^{i\sqrt{\pi}\theta_\rho} \cos\sqrt{\pi}\theta_\sigma). \quad (5.13)$$

In general, for a scattering potential  $V(x)$  with no special symmetry, the coefficients  $v_\rho$  and  $v_e$  will both be complex. For large  $v_\rho$ , the action will have deep minima when  $\theta_\rho$  is equal to a value  $\theta_{0\rho}$  determined by the phase of  $v_\rho$ . In the “mixed” phase (charge insulator and/or spin conductor) we can safely integrate out the massive fluctuations of  $\theta_\rho$  about this minima to obtain an effective action in terms of  $\theta_\sigma$ :

$$S = \frac{1}{g_\sigma} \sum_{i\omega_n} |\omega_n| |\theta_\sigma(\omega_n)|^2 + \int d\tau \mathcal{R}(v_e e^{i\sqrt{\pi}\theta_{0\rho}} \cos\sqrt{\pi}\theta_\sigma). \quad (5.14)$$

As (5.5) shows, the nonlinear term above flows to zero and is irrelevant when  $g_\sigma < 4$ , leaving a spin conductor. We therefore conclude that for a general scattering potential  $V(x)$ , the charge-insulator and/or spin-conductor phase is stable for  $g_\rho < 4$  and  $g_\sigma > 4$ . This is shown as the shaded region in Fig. 6(c).

When the scattering potential has an inversion symmetry,  $V(x) = V(-x)$ , though, we may choose both  $v_e$  and  $v_\rho$  to be real. It then follows that  $\sqrt{\pi}\theta_{0\rho} = \pi/2$  (provided  $v_\rho$  is positive, which corresponds to a potential barrier). Therefore, the coefficient of the  $\cos\sqrt{\pi}\theta_\sigma$  term in (5.14) vanishes identically. The next most relevant perturbation is  $v_\sigma$ , which becomes relevant only when  $g_\sigma < 1$ . Thus with inversion symmetry, the charge-insulator and/or spin-conductor phase is stable for all  $g_\rho < 4$  and  $g_\sigma > 1$ , as depicted by the cross-hatched region in Fig. 6(c). In particular, we find that for the physically interesting case with SU(2) symmetry ( $g_\sigma = 2$ ), this mixed phase can only be stable for a symmetric potential.

The spin-insulator and/or charge-conductor phase may be analyzed in a similar fashion by simply interchanging  $\rho$  and  $\sigma$  in the above equations. In the absence of SU(2) invariance, when  $V(\theta_\sigma) \neq V(-\theta_\sigma)$ , this phase is stable for  $g_\sigma < 4$  and  $g_\rho > 4$ , as shown in the shaded region of Fig. 6(d). When the barrier has spin symmetry, however, we have the analog of the inversion symmetry described above, and this phase is stable for  $g_\rho > 1$ , as shown in the cross-hatched region of Fig. 6(d).

### D. Intermediate-coupling fixed points and universal conductance

As discussed in Sec. V C above, for every value of  $g_\sigma$  and  $g_\rho$  at least one of the four possible phases (corresponding to charge and spin conducting or insulating) is stable. However, as is clear from inspection of Figs. 6(a)–6(d), there are values of  $g_\sigma$  and  $g_\rho$  for which more than one phase is stable. For example, there is a small region just to the right of  $g_\sigma = 3$  and  $g_\rho = 1$ , where for weak

backscattering the phase in which both spin and charge are perfectly transmitted is stable, whereas for a large barrier the perfectly reflecting or insulating phase is stable. It is clear that in this region there must exist a phase transition at finite barrier height separating these two phases.

In this section we show that it is possible to perturbatively access this nontrivial critical point both in the small- and large-barrier limits. We also evaluate the charge and spin conductance at this new critical point and find that it is universal, depending only on the lead conductances  $g_\sigma$  and  $g_\rho$ .

In the small-barrier limit the critical fixed point described above becomes perturbatively accessible near the point  $g_\sigma=3$  and  $g_\rho=1$ . The reason is that at these particular values both the  $2k_F$  electron backscattering, denoted  $v_e$ , and the backscattering of an up-spin and down-spin electron (together), denoted  $v_\rho$ , are marginal perturbations (see Fig. 6). For  $g_\sigma=3+\epsilon_\sigma$  and  $g_\rho=1+\epsilon_\rho$ , with small  $\epsilon$ 's, both  $v_e$  and  $v_\rho$ , when initially small, flow to zero with an eigenvalue proportional to  $\epsilon$ , as is clear from (5.5). We show below by performing a renormalization group to second order in  $v_e$  and  $v_\rho$  that there exists a critical fixed point separating these stable flows to zero coupling from flows to strong coupling, which presumably take one into the totally insulating phase. The fixed point, being at order  $\epsilon$ , is perturbatively accessible, and the critical properties can be directly computed.

To this end, consider the action in the  $\theta$  representation corresponding to a sum of the pure Luttinger-liquid action,  $S_0$  in (5.1), and the two types of weak backscattering,  $v_e$  and  $v_\rho$ :

$$S = S_0 + \int d\tau \mathcal{R}(v_e e^{i\sqrt{\pi}\theta_\rho} \cos\sqrt{\pi}\theta_\sigma + v_\rho e^{i2\sqrt{\pi}\theta_\rho}). \quad (5.15)$$

In general, for a scattering potential  $V(x)$  with no special symmetry, the coefficients  $v_e$  and  $v_\rho$  will both be complex. However, by shifting  $\theta_\rho$  by an appropriate constant, we can eliminate the imaginary part of  $v_e$ , leaving three independent real coupling constants,  $v_e$  and  $v_\rho = v_1 + iv_2$ .

The renormalization-group flow equations to second order are

$$dv_e/dl = - \left[ \frac{\epsilon_\rho + \epsilon_\sigma}{4} \right] v_e - v_1 v_e, \quad (5.16a)$$

$$dv_1/dl = -\epsilon_\rho v_1 - \frac{v_e^2}{4}, \quad (5.16b)$$

$$dv_2/dl = -\epsilon_\rho v_2, \quad (5.16c)$$

where we have  $g_\rho = 1 + \epsilon_\rho$  and  $g_\sigma = 3 + \epsilon_\sigma$ . Provided both  $\epsilon_\rho$  and  $\epsilon_\rho + \epsilon_\sigma$  are positive, these flow equations exhibit a critical fixed point at  $v_e^* = [\epsilon_\rho(\epsilon_\rho + \epsilon_\sigma)]^{1/2}$ ,  $v_1^* = -(\epsilon_\rho + \epsilon_\sigma)/4$ , and  $v_2^* = 0$ . As shown in Fig. 8, this fixed point separates flows toward strong coupling from flows to the origin. The correlation time exponent can be extracted as usual from the one relevant eigendirection at the critical fixed point.

There also exists a critical fixed point when  $\epsilon_\rho$  and

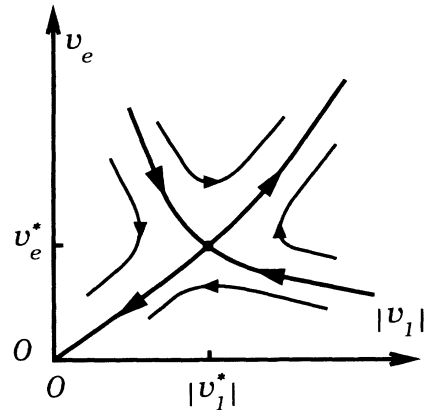


FIG. 8. Schematic renormalization-group flows for the transition between the insulating and conducting phases of an interacting electron gas with spin incident upon a barrier, as obtained from the flow equations (5.16). Here  $v_e$  denotes the strength of the  $2k_F$  electron backscattering, and  $v_1$  the real part of the amplitude for simultaneous  $2k_F$  backscattering of a spin-up and spin-down electron.

$\epsilon_\sigma + \epsilon_\rho$  are both negative. As we shall show in detail in Sec. VIA in connection with resonant tunneling, when the barrier is symmetric, this fixed point separates flows to different strong-coupling fixed points (namely the insulator and the charge insulator and/or spin conductor).

Before evaluating the conductance at this new critical fixed point, we show that it is also possible to access this transition in the large-barrier (i.e., small- $t$ ) limit. This is possible in the vicinity of the point  $g_\sigma=4$  and  $g_\rho=\frac{4}{3}$ , where we see from Eq. (5.10) that both  $t_e$  and  $t_\sigma$  are marginal perturbations. This point is the intersection of the two boundaries in the upper left part of Fig. 6(b). In this case, the action in the  $\phi$  representation following from (5.7) and (5.9) has the form

$$S = S_0 + \int d\tau t_e \cos\sqrt{2}\pi\phi_\sigma \cos 2\sqrt{\pi}\phi_\rho + t_\sigma \cos 4\sqrt{\pi}\phi_\sigma. \quad (5.17)$$

Formally, this is very similar to (5.15). Indeed, if we define  $g_\sigma=4-\tilde{\epsilon}_\sigma$  and  $g_\rho=\frac{4}{3}-\tilde{\epsilon}_\rho$ , the renormalization group flows to second order in  $t$  and can be deduced directly from (5.16):

$$dt_e/dl = - \left[ \frac{\tilde{\epsilon}_\sigma + 9\tilde{\epsilon}_\rho}{16} \right] t_e - t_e t_\sigma, \quad (5.18a)$$

$$dt_\sigma/dl = -\frac{\tilde{\epsilon}_\sigma}{4} t_\sigma - \frac{t_e^2}{4}. \quad (5.18b)$$

Provided  $\tilde{\epsilon}_\sigma$  and  $\tilde{\epsilon}_\sigma + 9\tilde{\epsilon}_\rho$  are both positive, there will be a critical fixed point at  $t_e^* = [\tilde{\epsilon}_\sigma(\tilde{\epsilon}_\sigma + 9\tilde{\epsilon}_\rho)]^{1/2}/4$  and  $t_\sigma^* = -(\tilde{\epsilon}_\sigma + 9\tilde{\epsilon}_\rho)/16$ . This fixed point separates flows to strong coupling (which presumably flow to the perfectly conducting fixed point) from flows to the origin (the insulating fixed point). It seems quite plausible that this fixed point, obtained in an expansion about  $g_\sigma=4$  and  $g_\rho=\frac{4}{3}$ , should match smoothly onto that found in (5.16) above in

the expansion about  $g_\sigma = 3$  and  $g_\rho = 1$ .

The conductance at these new critical fixed points to leading order may be obtained by simply plugging the fixed point values of the  $v$ 's or the  $t$ 's into the perturbative expressions derived in Appendix A. We have checked explicitly that this is legitimate by carrying out the perturbation theory for the conductance to third order in  $v$  and  $t$ , and verifying that all logarithmic divergences (in frequency) cancel at the fixed point. In the small- $v$  expansion (i.e., about  $g_\sigma = 3 + \epsilon_\sigma$  and  $g_\rho = 1 + \epsilon_\rho$ ) the conductance to lowest order in the  $\epsilon$ 's is

$$G^* = \frac{e^2}{h} \left[ (1 + \epsilon_\rho) - \frac{\pi^2}{16} (\epsilon_\sigma + \epsilon_\rho)(3\epsilon_\sigma + \epsilon_\rho) \right]. \quad (5.19)$$

Similarly, in the small- $t$  expansion (i.e.,  $g_\sigma = 4 - \tilde{\epsilon}_\sigma$  and  $g_\rho = \frac{4}{3} - \tilde{\epsilon}_\rho$ ) we find

$$G^* = \frac{e^2}{h} \frac{\pi^2}{32} \tilde{\epsilon}_\sigma (\tilde{\epsilon}_\sigma + 9\tilde{\epsilon}_\rho). \quad (5.20)$$

Additional critical fixed points may also be found in the vicinity of  $g_\rho = 3$ ,  $g_\sigma = 1$  and  $g_\rho = 4$ ,  $g_\sigma = \frac{4}{3}$ . The values of the  $t^*$ 's or  $v^*$ 's are identical to those above with  $\rho$  and  $\sigma$  interchanged, and the conductance at these fixed points again follows from the perturbation theory in Appendix A.

## VI. RESONANT TUNNELING OF ELECTRONS WITH SPIN

We now consider the problem of resonant transmission through a double barrier including a spin degree of freedom. The general structure of the problem is similar to that of the spinless case. That is, in the situation where there is only a single relevant perturbation about the conducting fixed point (e.g.,  $v_1$ ), it is possible, by tuning some parameter, to achieve the resonance condition that the renormalized value of  $v_1 = 0$ . In this case, there is perfect transmission on resonance.

There are, however, important differences regarding the nature of these resonances in the large-barrier limit. Specifically, when the barriers are large, so that the charge between them is discrete, there will be a spin degeneracy on the island when the charge is odd. This is reminiscent of the Kondo problem<sup>31</sup> in which a local moment is coupled to conduction electrons. This problem has recently been analyzed in some detail for the case of Fermi-liquid leads,<sup>17-19</sup> and it has been shown that there can be ‘‘Kondo resonances’’ with perfect transmission even when there is a Coulomb blockade fixing the charge on the island. We find that the Kondo resonances are the generic resonances for transmission through a double barrier, and for symmetric barriers can be achieved by tuning only a single parameter. Other ‘‘higher-order’’ resonances are also possible, but will in general require the fine tuning of more parameters and will therefore be difficult to ‘‘find’’ in practice. (One such case is a ‘‘charge’’ resonance where both the spin and charge states on the island are degenerate.) Again, we follow the same program of first analyzing the problem in the small-barrier limit and then the large-barrier limit.

### A. Small barriers

As we saw in Sec. IV A, for a spinless electron gas the condition for resonances was that the (fully renormalized)  $2k_F$  backscattering vanished. For a symmetric potential  $V(x)$ , this could be obtained by fine tuning a single parameter (e.g., the gate voltage), since the Fourier transform of  $V(x)$  is then real. More generally, however, two parameters would need to be tuned. With spin present, this reasoning still applies, and we obtain below the on-resonance phase diagram. As we shall see, for the physically relevant case with SU(2) spin symmetry (where  $g_\sigma = 2$ ), both charge and spin are perfectly transmitted on resonance, provided  $g_\rho > 1$ . For  $g_\rho < 1$ , the system flows to the phase in which the spin is still perfectly transmitted on resonance, but the charge is completely reflected.

In addition to this resonance, which we refer to as a ‘‘Kondo’’ resonance for reasons which will become apparent in the next section, there is another (intermediate-coupling) resonance which we have found which can also be accessed by tuning a single parameter [or two parameters when  $V(x)$  is not symmetric]. This latter resonance is of interest for two reasons: (i) On resonance, the charge and spin are not perfectly transmitted, as they are on the Kondo resonance. Rather, the charge and spin conductances are shown to take on universal values. (ii) With SU(2) spin symmetry, this ‘‘intermediate-coupling’’ resonance is present for  $g_\rho < 1$ , a regime in which the Kondo resonance is a charge insulator (and thus difficult to observe). We analyze this ‘‘intermediate-coupling’’ resonance in more detail below, after discussing the Kondo resonance.

In the small-barrier limit, the condition for the Kondo resonance is that the  $2k_F$  backscattering,  $v_e$  in (5.3), is tuned to zero. With SU(2) spin symmetry ( $g_\sigma = 2$ ) the next most relevant scattering term corresponds to the backscattering of both a spin-down and spin-up electron, denoted  $v_\rho$ , and is given explicitly in (5.6a). As (5.5) shows,  $v_\rho$  is irrelevant provided  $g_\rho > 1$ . In this case, both charge and spin will be perfectly transmitted on resonance, since the weak barrier scales to zero at low energies. For  $g_\rho < 1$ , though,  $v_\rho$  increases under the renormalization-group flows. At low energies, there is thus a large barrier for the transfer of charge across the junction. However, since  $v_\sigma$  is irrelevant for  $g_\sigma > 1$ , there is no barrier to the transfer of spin. It is thus natural to expect that we flow to the charge-insulator and/or spin-conductor phase described above in Sec. V C.

When there is SU(2) symmetry, so that  $g_\sigma = 2$ , we thus expect that on resonance we have a charge and spin conductor for  $g_\rho > 1$  and a charge insulator and/or spin conductor for  $g_\rho < 1$ . We shall see that this is also the case in the large-barrier limit. This is shown in Fig. 9.

For general values of  $g_\rho$  and  $g_\sigma$ , the behavior of the Kondo resonance can be easily deduced from similar reasoning. In this case we can have each of the four possible phases, as described in Sec. V, depending on  $g_\rho$  and  $g_\sigma$ . The phase diagram in the  $g_\sigma$ - $g_\rho$  plane is shown explicitly in Fig. 10.

We now consider the ‘‘intermediate-coupling’’ resonance that we mentioned at the beginning of this section.

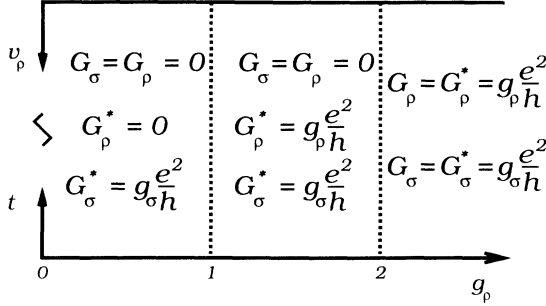


FIG. 9. Kondo-resonance phase diagram for interacting electrons with SU(2) spin symmetry,  $g_\sigma=2$ . Here  $G_\sigma$  and  $G_\rho$  denote off-resonance conductances, whereas the on-resonance conductances are denoted with an asterisk. The dashed line at  $g_\rho=2$  is the fixed line off resonance, while the dashed line at  $g_\rho=1$  is a fixed line on resonance.

This resonance arises from the competition between  $v_e$  and  $v_\rho$  in the situation when both are relevant perturbations. We therefore return to the action (5.15), in the  $\theta$  representation, keeping these terms:

$$S = S_0 + \int d\tau (v_e \cos\sqrt{\pi}\theta_\rho \cos\sqrt{\pi}\theta_\sigma) + \int d\tau (v_1 \cos 2\sqrt{\pi}\theta_\rho + v_2 \sin 2\sqrt{\pi}\theta_\rho), \quad (6.1)$$

where we have shifted  $\theta_\rho$  by a constant, so that now the  $2k_F$  backscattering  $v_e$  can be taken as real, and  $v_1$  and  $v_2$  are the real and imaginary parts, respectively, of  $v_\rho$ .

For simplicity, consider initially the SU(2) spin-symmetric case, with  $g_\sigma=2$ . Equation (5.5) shows that when  $g_\rho < 1$  all three coupling constants in (6.1) are relevant. Imagine for the moment setting  $v_e=0$ . Then under the flows of  $v_1$  and  $v_2$ , which scale off to strong coupling, the system enters a charge-insulating but spin-conducting phase. Is this phase stable to a small  $v_e$  term? In general, no, but as we discussed in Sec. VC, when the

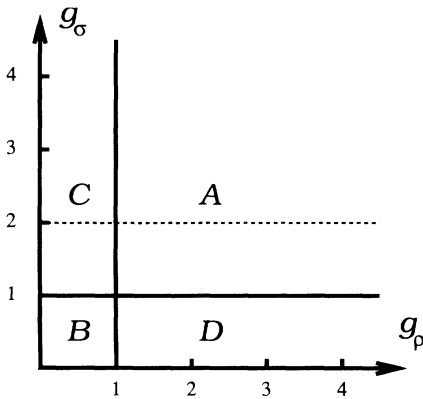


FIG. 10. Kondo-resonance phase diagram in the  $g_\rho$ - $g_\sigma$  plane, as obtained in the small-barrier limit from Eq. (5.5). The four phases are (A) charge and spin conductor, (B) charge and spin insulator, (C) charge insulator and/or spin conductor, (D) spin insulator and/or charge conductor. The dashed line indicates an electron gas with SU(2) spin symmetry.

potential  $V(x)$  is symmetric, so that  $v_2=0$  in (6.1), then this “mixed” phase is stable. The reason is that when  $v_1 \rightarrow \infty$  and  $v_2=0$ , up to small massive fluctuations, we can put  $2\sqrt{\pi}\theta_\rho=\pi$  in (6.1), which makes the term proportional to  $v_e$  vanish. On the other hand, when  $v_1=v_2=0$ , as  $v_e$  grows large under renormalization the system is expected to enter into a phase with both charge and spin insulating. It is thus clear that when  $v_2=0$  and  $g_\rho < 1$ , there should be a transition between these two phases as the ratio  $v_1/v_e$  is varied. As we shall see, precisely at this transition the charge conductance has a finite value. Since the two phases on either side of this transition are charge insulators, the transition is a charge resonance in the sense that as a parameter is tuned through the transition a peak in the charge conductance will occur.

In the SU(2) case, the “resonance” fixed point, which separates flows to these two phases, is at intermediate coupling and is therefore inaccessible perturbatively. However, we now show that by allowing  $g_\sigma$  to be different than 2 we can perturbatively access it. Recall that all three operators in (6.1) above are marginal when  $g_\rho=1$  and  $g_\sigma=3$ . This suggests an analysis similar to that in Sec. VD, perturbative in  $\epsilon_\rho=g_\rho-1$  and  $\epsilon_\sigma=g_\sigma-3$ . The analysis is identical to Sec. VD, except that now we consider  $\epsilon_\rho$  and  $\epsilon_\sigma+\epsilon_\rho$  to both be negative. Indeed, we can simply use again the second-order RG equations for  $v_e$ ,  $v_1$ , and  $v_2$ , given explicitly in (5.16). When both  $\epsilon_\rho$  and  $\epsilon_\sigma+\epsilon_\rho$  are negative, these flow equations give a critical fixed point at  $v_e^*=[\epsilon_\rho(\epsilon_\rho+\epsilon_\sigma)]^{1/2}$ ,  $v_1^*=|\epsilon_\rho+\epsilon_\sigma|/4$ , and  $v_2^*=0$ . The RG flows in the  $v_e$ - $v_1$  plane are sketched schematically in Fig. 11. The transition separates the “mixed” phase (charge insulator and/or spin conductor) from the totally insulating phase, as discussed above. At the critical fixed point,  $v_2$  is a relevant perturbation. This is consistent with the fact that for  $g_\sigma=3$  and  $g_\rho=1$ , the charge-insulator and/or spin-conductor “mixed” phase is only stable then the barrier is symmetric, so that  $v_2=0$ . The conductance at this resonance critical point can be evaluated by inserting the

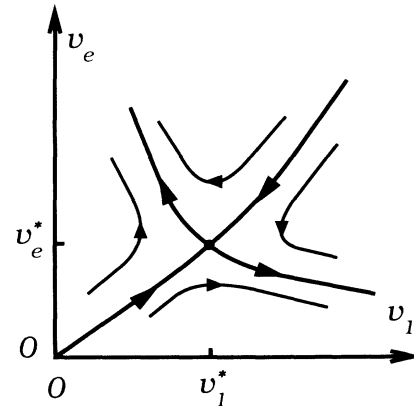


FIG. 11. Schematic renormalization-group flows describing the transition between the spin and charge insulator and the spin-conductor and/or charge-insulator phases, as described in Sec. VIA.

fixed-point values  $v_e^*$  and  $v_1^*$  into the general expressions derived in Appendix A, and to leading order in  $\epsilon$  the result is identical to (5.19).

### B. Large barriers: Kondo resonance

We now consider resonant tunneling with spin in the limit of large barriers. In this case, we again anticipate physics associated with the Coulomb blockade, which fixes the charge on the island. The spin degree of freedom gives the problem an additional twist, however, since when the charge on the island is an odd integer, there will be a spin degeneracy on the island in the absence of a magnetic field. This is analogous to the Kondo effect, where the island plays the role of the localized magnetic impurity. It has been shown that such a situation can give rise to a ‘‘Kondo’’ resonance in the transmission through the island.<sup>17–19</sup> Below we show that such a Kondo resonance can occur in a Luttinger liquid, and that it is the direct analog of the  $v_e=0$  resonance discussed in Sec. VIA above, in the small-barrier limit.

It is again instructive to consider first the special model with two equal strength  $\delta$ -function barriers, which we studied in Sec. IV B in connection with spinless electrons. Again, denoting the  $\theta_{\sigma,\rho}$  fields at the two barriers with subscripts 1 and 2, we define  $\theta_{\sigma,\rho}=(\theta_{1\sigma,\rho}+\theta_{2\sigma,\rho})/2$ , and  $n_{\sigma,\rho}=(\theta_{2\sigma,\rho}-\theta_{1\sigma,\rho})/\sqrt{\pi}$ . Physically,  $\theta_{\sigma,\rho}/\sqrt{\pi}$  correspond to the spin and charge which have been transferred across the junction, and thus play a role similar to the  $\theta$  fields which entered into the single-barrier problem, (5.1)–(5.4). Moreover,  $n_{\sigma,\rho}$  may be interpreted as the spin and the charge between the two barriers. The low-frequency effective potential analogous to (4.2) experienced by  $\theta_{\sigma,\rho}$  and  $n_{\sigma,\rho}$  then has the form

$$V_{\text{eff}} = V \left[ \cos\sqrt{\pi}\theta_\rho \cos\sqrt{\pi}\theta_\sigma \cos\frac{\pi}{2}n_\rho \cos\frac{\pi}{2}n_\sigma + \sin\sqrt{\pi}\theta_\rho \sin\sqrt{\pi}\theta_\sigma \sin\frac{\pi}{2}n_\rho \sin\frac{\pi}{2}n_\sigma \right] + \frac{U_\rho}{2}(n_\rho - n_{0\rho})^2 + \frac{U_\sigma}{2}(n_\sigma - n_{0\sigma})^2. \quad (6.2)$$

Here  $V$  is the strength of the two  $\delta$ -function scatterers, and the  $U$ 's suppress charge and spin fluctuation on the ‘‘island’’ between the two barriers. Again,  $n_{0\rho}$  can be tuned by varying a gate voltage  $V_G$ . In the case with SU(2) spin symmetry,  $n_{0\sigma}=0$ .

As in Sec. IV B, we analyze the symmetries of this model. It is clear that Eq. (6.2) is invariant under the transformation  $\theta_\rho \rightarrow \theta_\rho \pm \sqrt{\pi}$  and  $\theta_\sigma \rightarrow \theta_\sigma \pm \sqrt{\pi}$ . This corresponds to transporting an electron from the right to the left leads, and is related to the single-particle hopping term  $t_e$ . As in the spinless case, we shall see that resonance is possible when there is an additional symmetry. In the absence of a magnetic field (when  $n_{0\sigma}=0$ ), such a symmetry exists when  $n_{0\rho}$  is an *odd* integer. In this case  $V_{\text{eff}}$  is invariant under the additional transformation  $n_\sigma \rightarrow -n_\sigma$ ,  $n_\rho \rightarrow 2n_{0\rho} - n_\rho$  in conjunction with *either*

$\theta_\rho \rightarrow \theta_\rho + \sqrt{\pi}$  or  $\theta_\sigma \rightarrow \theta_\sigma + \sqrt{\pi}$ . These transformations correspond physically to processes where (i) an electron is transferred across the island flipping its own spin and that of the island, or (ii) an electron in one lead flips its spin and the spin on the island.

In the limit  $V \ll U_\rho, U_\sigma, n_\rho$ , and  $n_\sigma$  may be integrated out, leaving a model similar to (5.4). However, in the presence of the additional symmetry above (when  $n_{0\rho}$  is an odd integer), the effective potential  $V_{\text{eff}}(\theta_\sigma, \theta_\rho)$ , which enters in (5.4), now has an additional symmetry, namely invariance under either  $\theta_\sigma \rightarrow \theta_\sigma + \sqrt{\pi}$  or  $\theta_\rho \rightarrow \theta_\rho + \sqrt{\pi}$ . This means that the  $2k_F$  electron backscattering term in (5.4),  $v_e \cos 2\sqrt{\pi}\theta_\sigma \cos 2\sqrt{\pi}\theta_\rho$ , is not allowed. But the vanishing of  $v_e$  was precisely the condition for resonance in the small-backscattering limit.

In the limit of large barriers, on the other hand,  $V_{\text{eff}}$  in (6.2) will have deep minima when  $n_\rho$  and  $n_\sigma$  are integers. When the resonance condition defined above is satisfied, there are then two degenerate spin states, which have  $n_\sigma = \pm 1$ , respectively. This is reminiscent of the Kondo effect, in which a local moment is coupled to conduction electrons. For this reason, we refer to this resonance as a ‘‘Kondo’’ resonance.

The partition function on resonance will be dominated by instantons connecting the various degenerate minima of  $V_{\text{eff}}$  related by the symmetries described above. The fugacity of the instanton corresponding to the process in which an electron hops across the island leaving the spin on the island unchanged is denoted by  $t_e$ . It should be clear that this has the same physical content as that defined in Sec. V, namely a single electron hopping from the left to right leads. Similarly, the fugacities of the instantons corresponding to processes (i) and (ii) described above, in which the spin on the island is flipped, are denoted by  $\tilde{t}_\rho$  and  $\tilde{t}_\sigma$ , respectively. These two processes are distinct from  $t_\sigma$  and  $t_\rho$  defined in Sec. V.

As in Sec. IV B, we can analyze the effects of these processes with a renormalization-group approach. To this end, we define  $q_i = \Delta\theta_\rho/\sqrt{\pi}$  and  $s_i = \Delta\theta_\sigma/\sqrt{\pi}$ , which, as in (5.12), measure the charge and spin transferred to the right. In addition, in order to specify fully all of the allowed processes, we must define  $t_i = \Delta n_\sigma/2$  as the change of the spin on the island. With these definitions, the hopping of a single electron between leads,  $t_e$ , corresponds to  $(q_i, s_i, t_i) = (\pm 1, \pm 1, 0)$ , whereas the  $\tilde{t}_\rho$  process corresponds to  $(\pm 1, 0, \pm 1)$  and the  $\tilde{t}_\sigma$  process to  $(0, \pm 1, \pm 1)$ . While  $q_i$  and  $s_i$  can have any ordering,  $t_i$ , which is constrained by the allowed spin states on the island, must alternate in sign.

By expanding the partition function in powers of  $t_e, \tilde{t}_\rho$ , and  $\tilde{t}_\sigma$ , we arrive at a Coulomb-gas model, where now the interaction between the ‘‘charges’’ has the form

$$V_{ij} = \left[ \frac{2}{g_\rho} q_i q_j + \frac{2}{g_\sigma} (s_i s_j + K_\sigma t_i t_j) \right] \ln(\tau_i - \tau_j) / \tau_c. \quad (6.3)$$

Notice that this differs from the single-barrier expression (5.12) by the presence of the term proportional to  $K_\sigma$ . Here in the double-barrier case we have initially  $K_\sigma = 1$ ,

but, as we shall see, its value is reduced upon renormalization. Specifically, upon applying the real-space renormalization-group procedure used in Sec. IV B, we arrive at the following RG flow equations to leading order in the hopping strengths ( $t$ 's):

$$d\tilde{t}_\rho/dl = \left[ 1 - \frac{1}{g_\rho} - \frac{K_\sigma}{g_\sigma} \right] \tilde{t}_\rho, \quad (6.4a)$$

$$d\tilde{t}_\sigma/dl = \left[ 1 - \frac{1}{g_\sigma}(1+K_\sigma) \right] \tilde{t}_\sigma, \quad (6.4b)$$

$$dt_e/dl = \left[ 1 - \frac{1}{g_\rho} - \frac{1}{g_\sigma} \right] t_e, \quad (6.4c)$$

$$dK_\sigma/dl = -8(\tilde{t}_\rho^2 + \tilde{t}_\sigma^2)\tau_c^2 K_\sigma. \quad (6.4d)$$

The structure of these equations is similar to that of (4.5) for the resonant tunneling of spinless electrons. The resulting phase diagram for the case with SU(2) spin symmetry ( $g_\sigma=2$ ) is shown in Fig. 9. In this case, since  $K_\sigma$  is always less than 1,  $\tilde{t}_\sigma$  always grows under the flows and we expect perfect spin transmission, regardless of the value of  $g_\rho$ . For attractive interactions,  $g_\rho > 2$ , both  $t_e$  and  $\tilde{t}_\rho$  will also grow under the RG flows and so charge is also expected to be perfectly transmitted (in this case a single barrier conducts perfectly). For repulsive interactions with  $g_\rho$  in the range,  $1 < g_\rho < 2$ , although  $t_e$  will initially decrease, after  $K_\sigma$  flows to zero, the charge hopping  $\tilde{t}_\rho$  will grow. We thus expect that in this case also, both charge and spin will be perfectly transmitted on resonance, even though a single barrier will be insulating. For  $g_\rho < 1$ , on the other hand,  $\tilde{t}_\rho$  and  $t_e$  will both flow to zero, so that the system is presumably insulating. However, since  $\tilde{t}_\sigma$  continues to grow even in this case, we expect the phase to be a charge insulator and/or spin conductor.

As in the spinless case, the decreases in  $K_\sigma$  under renormalization may be understood as an effective decrease in the ratio  $V/U$  in (6.2), and indicates that the discreteness of charge and spin on the island has become less important. When  $K_\sigma$  flows completely to zero, we are left with an effective single-barrier problem, except that now, since we have the additional symmetry under  $\theta_\sigma \rightarrow \theta_\sigma + \sqrt{\pi}$  or  $\theta_\rho \rightarrow \theta_\rho + \sqrt{\pi}$ , processes in which a “charge” hops without a “spin” or vice versa are allowed. This corresponds precisely to the small-barrier limit, provided one tunes to resonance with  $v_e=0$ . We can thus identify the small-barrier resonance (when  $v_e=0$ ), with the Kondo resonance which we have analyzed in the large-barrier limit.

Allowing for more general values of  $g_\sigma$ , we can construct the Kondo resonance phase diagram in the small- $t$  limit directly from (6.4), since in this limit the  $t$ 's flow to zero before  $K_\sigma$  changes appreciably, so that the boundaries are determined with  $K_\sigma=1$ . In Fig. 12 we display this phase diagram as a function of  $g_\sigma$  and  $g_\rho$ . The phase boundary at  $g_\rho=4$  is determined by the relevance of  $t_\rho$ , which is not included in (6.4) (see Sec. V B). For larger values of the initial hopping strengths  $t$ , the phase boundaries will shift, since then  $K_\sigma$  has “time” to flow. If  $K_\sigma$

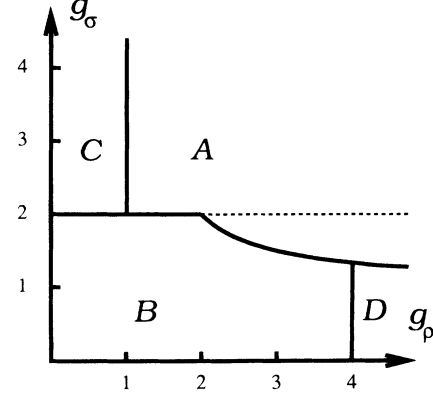


FIG. 12. Kondo-resonance phase diagram in the  $g_\rho$ - $g_\sigma$  plane in the limit of large barriers, as obtained from the flow equations (6.4). The four phases are (A) charge and spin conductor, (B) charge and spin insulator, (C) charge insulator and/or spin conductor, (D) spin insulator and/or charge conductor. The dashed line indicates an electron gas with SU(2) spin symmetry.

flows all the way to zero, then the phase diagram becomes identical to that in the small-barrier limit displayed in Fig. 10.

In addition to the Kondo resonance described above, one might expect to have a “charge” resonance, which occurs when the gate voltage is adjusted to the point where the cost in energy to add another particle to the island vanishes identically. This is a direct analog of the resonance in the spinless case described in Sec. IV. In general, however, as we now point out, such a resonance will be more difficult to observe with spin, since it requires the tuning of more parameters. It is important to remember that simply adjusting the chemical potential of the island to the point where the energy to add another electron vanishes is generally not a sufficient condition for resonance. We saw this in Sec. IV, where we found that if the two barriers have even slightly different strengths, the resonance is ultimately destroyed. (This is in contrast to what occurs for noninteracting electrons.) Specifically, in this case, an asymmetry in the barrier strengths will break the “resonance symmetry” of the effective potential  $V_{\text{eff}}$  in (4.2).

In the case with spin, two adjacent charge states of the island will become degenerate in energy when  $n_{0\rho}$  in (6.2) is tuned to be a half-integer. However, (6.2) does not possess any extra “resonance symmetry” unless, in addition,  $n_{0\sigma}$  is also tuned to be a half-integer. (This will not generally be the case even in a magnetic field.) If this can be achieved, though, then (6.2) will be invariant when both  $n_\sigma$  and  $n_\rho$  change by  $\pm 1$  and both  $\theta_\sigma$  and  $\theta_\rho$  change by  $\pm\sqrt{\pi}/2$ . This corresponds physically to hopping an electron from one of the leads onto the island, which is what we expect for the “charge” resonance. If we trace this symmetry to the small-barrier limit, as was done above for the Kondo resonance, then we find that  $V_{\text{eff}}(\theta_\sigma, \theta_\rho)$  must be invariant under the combined transformation  $\theta_\sigma \rightarrow \theta_\sigma \pm \sqrt{\pi}/2$  and  $\theta_\rho \rightarrow \theta_\rho \pm \sqrt{\pi}/2$ . This requires that in addition to  $v_e=0$ , we must also have  $v_\sigma=v_\rho=0$ . Thus this is clearly a “higher-order” resonance, which requires



the tuning of six parameters. Evidently, the effective potential (6.2) has some extra symmetry built into it, which allowed us to achieve this resonance tuning only two parameters  $n_{0\rho}$  and  $n_{0\sigma}$ . There is no reason to expect that such a symmetry should be present in a more general potential.

## VII. RESONANCE LINE SHAPES

The above discussion has focused on the conductance through a double barrier when precisely on resonance and at  $T=0$ . A more crucial issue experimentally is the width of the resonances and the line shapes of the resonance peaks. Consider then the regions in the phase diagrams (Figs. 3 and 9 for spinless and spinful electrons, respectively) where resonances with perfect transmission occur when some parameter, such as a gate voltage, is tuned. Precisely on resonance, the RG flows are toward the fixed point which describes the pure Luttinger liquid with no scattering, i.e., that given in (3.3). Since all scattering except the  $2k_F$  scattering is irrelevant at this fixed point, the resonance condition is that the *renormalized* value of  $V(2k_F)=0$ . As the system is tuned slightly off resonance, by, for example, changing the chemical potential, the conductance will be determined by the behavior of this single relevant parameter as it flows away from that unstable fixed point. Near resonance, the initial value of this parameter will be proportional to the distance from resonance,  $V(2k_F, l=0) \approx \delta \equiv V_G - V_G^*$ . Under renormalization, the  $2k_F$  scattering grows, as  $dv_1/dl = \lambda v_1$ , with a positive eigenvalue, denoted as  $\lambda$ , given by

$$\lambda = 1 - g \quad (7.1a)$$

for spinless electrons and

$$\lambda = 1 - (g_\sigma + g_\rho)/4 \quad (7.1b)$$

for electrons with spin. As usual near a critical point, we can introduce a divergent time scale associated with this relevant direction which diverges as  $\delta \rightarrow 0$  as  $\delta^{-1/\lambda}$ . From this we deduce a characteristic frequency scale, denoted  $\Omega$ , which vanishes as  $\Omega \approx \delta^{1/\lambda}$ . Near the resonance for small  $\delta$  the conductance at finite temperatures should depend only on the ratio  $k_B T / \hbar \Omega$ . More specifically, one expects the conductance for small  $T$  and  $\delta$  to be described by a *universal scaling function*:

$$G(T, \delta) = \tilde{G}_g(c\delta/T^\lambda), \quad (7.2)$$

where  $c$  is a nonuniversal dimensionful constant. For larger  $\delta$  or  $T$ , the irrelevant parameters will provide corrections to this scaling form. For instance, for the spinless case there will also be a dependence in (7.2) on  $V(4k_F)T^{(4g-1)}$ , which, however, vanishes in the zero-temperature limit.

The scaling function  $\tilde{G}_g(X)$ , which is a symmetric function of its argument,  $X = c\delta/T^\lambda$ , can be obtained for small  $X$  directly from our perturbative results in Sec. III A, Eq. (3.5) and Sec. V A, Eq. (5.6). We find a quadra-

tic dependence,

$$\tilde{G}_g(X) = G^*[1 - X^2 + O(X^4)], \quad (7.3)$$

where the conductance on resonance is  $G^* = ge^2/h$  for the spinless case and  $G^* = g_\rho e^2/h$  for electrons with spin. The behavior of  $\tilde{G}_g$  for large  $X$  can be obtained by matching onto the flows into the stable fixed point which describes reflection from a single large barrier. As shown in Secs. III B and V B, off resonance (e.g., for a single barrier) the conductance vanishes as  $G \approx t^2 T^{2(1/g-1)}$  for spinless electrons and as  $G \approx t^2 T^{2/g_\rho-1}$  with spin. Requiring that the form in (7.2) matches onto this implies that as  $X \rightarrow \infty$ ,

$$\tilde{G}_g(X) \approx X^{-2/g} \quad (7.4a)$$

for the spinless case and

$$\tilde{G}_{g_\rho}(X) \approx X^{-4/g_\rho} \quad (7.4b)$$

for electrons with spin. For intermediate values of  $X$ , although  $\tilde{G}_g(X)$  is not perturbatively accessible, it should be a universal function, depending only on the dimensionless lead conductance  $g$  or  $g_\rho$ . In the next section we will indeed verify this for the spinless case with  $g = \frac{1}{2}$ , where an exact nonperturbative solution is possible.

The above considerations show that at low temperatures the resonance peaks should have a temperature-dependent width which scales as  $T^\lambda$ . Moreover, rescaled data from different temperatures should collapse onto the same universal curve. The line shapes of the peaks are predicted to be *non-Lorentzian*, with tails which fall off as  $\delta^{-2/g}$  in the spinless case and as  $\delta^{-4/g_\rho}$  with spin. In both cases, the line shape is Lorentzian and temperature independent in the limit of noninteracting electrons ( $g=1$  and  $g_\rho=2$ ), as expected.

For a 1D channel with a finite length  $L$ , which is joined at the ends to metallic (Fermi-liquid) leads, the predicted power-law behavior will be cut below a temperature  $T_L = \hbar v_F / k_B L$ . Specifically, the resonance line shapes will cease to sharpen up below this crossover temperature. In addition, at low temperatures a finite applied voltage will serve as a cutoff. Thus, at  $T=0$ , the  $I$ - $V$  curves near resonance (for  $V > k_B T_L / e$ ) should satisfy a scaling form,  $I/V = \tilde{G}_g^V(\delta/V^\lambda)$ . Although  $\tilde{G}_g^V(X)$  should be a *universal* function with the same small- and large- $X$  dependences as  $\tilde{G}_g(X)$  in (7.3), the two functions will in general be different.

When the barriers are asymmetric, it is likely that as the gate voltage  $V_G$  is tuned, we do not pass through the resonance point  $V(2k_F)=0$ . However, if the asymmetry is not too large, it is likely that there exists a well-defined minimum  $\delta_{\min} = \min|V(2k_F)|$  at some value  $V_G^*$ . In this situation,  $\delta$  in Eq. (7.2) should be replaced by  $f(\delta)$ , where for large  $\delta$   $f(\delta) = \delta$ , whereas for  $\delta \rightarrow 0$ ,  $f(\delta) \rightarrow \delta_{\min}$ . The resonance peak will then ultimately vanish at zero temperature, but at finite temperatures it will have a temperature dependence determined by  $G^* = \tilde{G}_g(c\delta_{\min}/T^\lambda)$ . Again, for temperatures below  $T_L$ ,  $T$  should be replaced by  $T_L$ .

### VIII. EXACT SOLUTION AT $g = \frac{1}{2}$

One of the beautiful features of scaling is that one often can extract a lot of information with relatively little effort. Indeed, in the previous section we inferred the temperature dependence of resonance widths and the asymptotic form of the resonance tails by simply piecing together the perturbative results of Secs. III and IV. A drawback of scaling, though, is that one is never quite certain about its validity in any particular case. Fortunately, as we now show, for spinless electrons with a particular value of the dimensionless conductance,  $g = \frac{1}{2}$ , the conductance through a resonance can be calculated exactly, with no recourse to perturbative methods. This solution follows closely a paper by Guinea,<sup>32</sup> where he obtained an exact solution of a closely related model which he was studying in the context of macroscopic quantum tunneling in Josephson junctions. Here we briefly outline his route to the solution, which ultimately involves mapping the problem into the 2D classical Ising model with a surface boundary condition. This enables us to extract the conductance as a function of temperature throughout the resonance regime, and verify both the perturbative results of Secs. III and IV, and, more importantly, the scaling results of Sec. VI.

The action we wish to solve is that for spinless interacting electrons in the presence of a  $2k_F$  backscattering term from a potential scatterer localized near  $x=0$ . In terms of the boson field  $\theta(x=0, \tau)$  the appropriate effective action follows from (3.2) and (3.3) and takes the form

$$S = \frac{1}{g} \sum_{i\omega_n} |\omega_n| |\theta(\omega_n)|^2 + v \int d\tau \cos[2\sqrt{\pi}\theta(\tau)], \quad (8.1)$$

where the coefficient  $v$  is proportional to the  $2k_F$  backscattering,  $\hat{V}(2k_F)$ . In arriving at (8.1) we have integrated out the fluctuations of  $\theta$  in the two leads, which generates the singular frequency dependence in the first term. It is, of course, the nonlinearity coming from the cosine term which makes this problem difficult to solve.

As noted by Guinea, when  $g = \frac{1}{2}$  we can write down a simple spin Hamiltonian which describes the same low-energy physics as (8.1) above. To be explicit, consider the following spin- $\frac{1}{2}$  quantum  $xy$  model defined on a semi-infinite lattice:

$$H = -\frac{1}{8} \sum_{n=0}^{\infty} (\sigma_n^+ \sigma_{n+1}^- + \text{H.c.}) + v \sigma_0^x, \quad (8.2)$$

where  $\sigma$  is a spin-one-half operator, and as usual  $\sigma^\pm = \sigma^x \pm i\sigma^y$ . The last term is a “magnetic field” acting on the end site. To establish the equivalence between (8.2) and (8.1) it is useful to note that the  $xy$  model can be mapped into a fermion model using a Jordan-Wigner transformation. The first term in (8.2) becomes simply the kinetic energy for noninteracting electrons hopping on a semi-infinite lattice. In the  $\phi$  representation the effective low-energy action for this term takes the form

$$S_0 = \frac{1}{2} \int_0^\infty dx \int d\tau (\partial_\mu \phi)^2, \quad (8.3a)$$

where we have used (2.4b) and have specialized to the

case  $g = 1$  appropriate for noninteracting electrons. Notice that in (8.3a) the  $x$  integration is restricted to positive  $x$ , as appropriate for the semi-infinite system under consideration. The second term, when expressed in terms of the fermion field  $\psi_n$ , is of the form  $\psi_0 + \psi_0^+$ . Upon using (2.2) to bosonize this term and noting that since we are at the end of a semi-infinite lattice we can set  $\theta(x=0)=0$ , this term becomes

$$S_1 = v \int d\tau \cos[\sqrt{\pi}\phi(x=0, \tau)]. \quad (8.3b)$$

Upon integrating out  $\phi(x)$  away from  $x=0$ , in the semi-infinite lead, the first term (8.3a) becomes

$$S_0 = \frac{1}{2} \sum_{i\omega_n} |\omega_n| |\phi(\omega_n)|^2. \quad (8.4)$$

The equivalence is now clear. When we let  $\phi(\tau) \rightarrow 2\theta(\tau)$  in (8.3) and (8.4), the total action  $S_0 + S_1$  becomes identical to  $S$  in (8.1) provided  $g = \frac{1}{2}$ .

Before sketching Guinea’s solution to the spin problem in (8.2) it is useful to express the conductance in terms of the spin operator. To this end we add to the original action in (8.1) a source term of the form

$$\delta S = \frac{1}{\sqrt{\pi}} \int d\tau ia(\tau) \partial_\tau \theta(\tau), \quad (8.5)$$

which enables us to evaluate the conductance via two functional derivatives with respect to the “vector potential”  $a(\tau)$ ; see (2.9). Before taking these derivatives, though, it is convenient to perform a shift,  $\theta(\tau) \rightarrow \theta(\tau) + (g/2\sqrt{\pi})a(\tau)$ , which eliminates the term linear in  $a$  and gives for the full action,  $S_{\text{tot}} = S + \delta S$ ,

$$S_{\text{tot}} = \frac{1}{g} \sum_{i\omega_n} |\omega_n| |\theta(\omega_n)|^2 + v \int d\tau \cos[2\sqrt{\pi}\theta(\tau) + ga(\tau)] + \frac{g}{4\pi} \sum_{i\omega_n} |\omega_n| |a(\omega_n)|^2. \quad (8.6)$$

Upon differentiation twice with respect to  $a(\tau)$  we generate two contributions, one a constant piece coming from the last term in (8.6), and the other a correlation function of an operator,  $\hat{O} = \sin(2\sqrt{\pi}\theta)$ . Specifically, in an imaginary time representation the conductance is given by

$$G = \frac{ge^2}{h} + \frac{(gev)^2}{\hbar\omega_n} P(\omega_n), \quad (8.7a)$$

where

$$P(\omega_n) = \int_0^\beta d\tau (e^{i\omega_n\tau} - 1) P(\tau), \quad (8.7b)$$

$$P(\tau) = \langle T_\tau \hat{O}(\tau) \hat{O}(0) \rangle. \quad (8.7c)$$

Here  $\omega_n = 2\pi n/\beta$  is a Matsubara frequency. As usual, to get the dc conductance an analytic continuation to real frequencies must be performed,  $\omega_n \rightarrow -i\omega + \epsilon$ , before taking the zero-frequency limit. Finally, we need to express the operator  $\hat{O}$  in terms of the spin operators in the Hamiltonian (8.2). Since the mapping takes

$\sigma_0^+ \rightarrow \exp[i2\sqrt{\pi}\theta(\tau)]$  we have simply

$$\hat{O} = \sigma_0^y. \quad (8.7d)$$

We now briefly sketch Guinea's exact solution of the spin- $\frac{1}{2}$   $xy$  model in (8.2). This basically involves a sequence of mappings to bring the Hamiltonian into the quadratic form of fermions. First, it is convenient to perform a "duality" transformation from the original spin- $\frac{1}{2}$  operator  $\sigma$  to a dual spin- $\frac{1}{2}$  operator denoted  $\mu$ :

$$\sigma_n^x = \prod_{m \leq n} \mu_m^z, \quad (8.8a)$$

$$\sigma_n^y = \mu_n^x \mu_{n+1}^x. \quad (8.8b)$$

It is straightforward to check that the new operators  $\mu$  satisfy the appropriate spin commutation relations. The mapping in (8.8) has been used widely in the context of 1D quantum Ising models.<sup>33</sup> In terms of these new operators the Hamiltonian (8.2) becomes

$$H = -\frac{1}{4} \sum_{n=0}^{\infty} (\mu_n^x \mu_{n+2}^x + \mu_{n+1}^z) + v \mu_0^z. \quad (8.9)$$

In this representation, the model splits into two decoupled models, one on the even and the other on the odd sites,  $H = H_{\text{even}} + H_{\text{odd}}$ . Moreover, these two Hamiltonians clearly commute. Each model describes a semi-infinite quantum Ising model in a transverse field, with a free boundary condition on the end for the odd-site model, and a different field, of strength  $v$ , on the end site of the even-site model. It turns out that since the transverse field has identical strength to the Ising coupling term, the two models are at bulk critical points. As shown originally by Lieb, Schultz, and Mattis,<sup>34</sup> this critical point is in the 2D classical Ising model universality class. Thus (8.9) describe two decoupled semi-infinite 2D Ising models at criticality, one with a free boundary and the other with a boundary field given by  $v$ .

Since the Hamiltonian on the odd sites can be obtained from the even-site Hamiltonian via  $H_{\text{odd}} = H_{\text{even}}(v = -\frac{1}{4})$ , we need only solve the even-site problem. This can be achieved by mapping  $H_{\text{even}}$  into a free fermion model by performing a Jordan-Wigner transformation,

$$\mu_n^+ = 2c_n^+ \exp \left[ i\pi \sum_{m < n} c_m^\dagger c_m \right], \quad (8.10a)$$

$$\mu_n^z = \omega c_n^\dagger c_n - 1. \quad (8.10b)$$

Here  $c_n$  is a standard fermion operator and the sites  $n$  and  $m$  are even sites only. In terms of the fermion fields the Hamiltonian is quadratic,

$$H_{\text{even}} = -\frac{1}{4} \sum_{n=2}^{2(N+1)} [(c_{n-2}^\dagger - c_{n-2})(c_n^\dagger + c_n) + 2c_n^\dagger c_n] + 2vc_0^\dagger c_0, \quad (8.11)$$

where the sum is only over even sites. This can be brought into a diagonal form,

$$H_{\text{even}} = \sum_k E_k c_k^\dagger c_k, \quad (8.12)$$

with the  $k$  sum over  $k = \pi l / 2N$  with  $l = 1, 2, \dots, N$ , by using a Bogoliubov transformation,

$$c_k^\dagger = \frac{1}{\sqrt{8N}} \sum_{n=0,2,4,\dots}^{2N} [A_k^n (c_n^\dagger + c_n) + B_k^n (c_k^\dagger - c_n)], \quad (8.13)$$

provided the coefficients  $A_k^n$  and  $B_k^n$  are chosen correctly. Following Guinea's Appendix<sup>32</sup> we find that  $E_k = \sin(k)$ , and the coefficients are given by

$$A_k^0 = \frac{4v \cos(k)}{\exp(ik)E_k - 8iv^2}, \quad (8.14a)$$

$B_k^0 = E_k A_k^0 / 2v$  and for  $n = 2, 4, 6, \dots$

$$A_k^n = i^{n-1} e^{ik(n-1)} - (A_k^0 / A_k^{0*}) i^{n-1} e^{-ik(n-1)}, \quad (8.14b)$$

$$B_k^n = i^n e^{ikn} + (A_k^0 / A_k^{0*}) i^n e^{-ikn}. \quad (8.14c)$$

The inverse transformation to (8.13) is

$$ic_n^\dagger = \frac{1}{\sqrt{8N}} \sum_k [(A_k^n + B_k^n) c_k^\dagger + (A_k^{n*} - B_k^{n*}) c_k]. \quad (8.15)$$

It is now straightforward to evaluate  $P(\tau)$  in (8.7c), since it factorizes into a product of contributions from the even and odd sublattices,  $P(\tau) = P_{\text{even}}(\tau) P_{\text{odd}}(\tau)$ , where  $P_{\text{even}}(\tau) = \langle \hat{O}_{\text{even}}(\tau) \hat{O}_{\text{even}}(0) \rangle$  and  $\hat{O}_{\text{even}} = c_0^\dagger + c_0$ . At temperature  $T$  we find

$$P_{\text{even}}(\tau) = \frac{1}{\pi^2} \int_0^{\pi/2} dk |A_k^0|^2 [e^{-E_k \tau} (1 - f_{E_k}) + e^{E_k \tau} f_{E_k}], \quad (8.16)$$

where  $f_E = [\exp(\beta E) + 1]^{-1}$  is the Fermi function.  $P_{\text{odd}}(\tau)$  is given by this same expression except with  $v \rightarrow -\frac{1}{4}$ .

Upon combining (8.14a) and (8.16), then inserting into (8.7b) and performing the time integration, we find

$$P(\omega_n) = \frac{1}{(\pi v)^2} \int dE dE' \frac{(1-f_E)(1-f_{E'})}{1+(E/8v^2)^2} \times \frac{e^{-\beta(E+E')} - 1}{i\omega_n - (E+E')}, \quad (8.17)$$

where for small  $T$  and  $v$  the energy integrals can be taken from minus infinity to infinity. We are now in a position to perform the analytic continuation to real times, by letting  $i\omega_n \rightarrow \omega + i\epsilon$  in (8.17). After performing the integral over  $E'$  we then find in the zero-frequency limit

$$\lim_{\omega \rightarrow 0} \frac{\text{Im} P_R(\omega)}{\omega} = \frac{1}{(\pi v)^2} \int dE \frac{\partial f_E / \partial E}{1+(E/8v^2)^2}, \quad (8.18)$$

where  $P_R(\omega)$  denotes the retarded correlation function. Finally, upon inserting into (8.7a) we get the final result for the dc conductance at finite temperatures:

$$G(T, v) = \frac{e^2}{2h} \left[ 1 - \int_{-\infty}^{\infty} dE (-\partial f_E / \partial E) \frac{(8v^2)^2}{E^2 + (8v^2)^2} \right]. \quad (8.19)$$

Notice that in the presence of  $2k_F$  backscattering,

$v \neq 0$ , as the temperature tends to zero the conductance vanishes, since the Fermi function derivative is simply a  $\delta$  function of energy in this limit. The link is insulating at zero temperature regardless of how small the backscattering. Thus this nonperturbative result confirms the conclusions reached in Secs. III and IV, which were based upon piecing together perturbative results. If we take the backscattering to zero, to place us on resonance, and then take the temperature to zero, the conductance is given by  $G = G^* = e^2/2h$ , which corresponds to perfect transmission for the  $g = \frac{1}{2}$  case under consideration.

The exact result (8.19) can, moreover, be cast in the scaling form, given in (7.2), namely

$$G(T, v) = \tilde{G}_g(cv/T^{1-g}). \quad (8.20)$$

Upon comparing (8.19) and (8.20) we obtain an explicit expression for the scaling function at  $g = \frac{1}{2}$ :

$$\tilde{G}_{g=1/2}(X) = G^* \int_{-\infty}^{\infty} dy \frac{e^y}{(e^y + 1)^2} \frac{y^2}{y^2 + X^4}. \quad (8.21)$$

This scaling function has the predicted forms, deduced from the perturbative considerations of Secs. III and IV, namely quadratic deviations from  $G^*$  at small argument, and an  $X^{-2/g} \approx X^{-4}$  dependence for large argument. Thus, in summary, the exact solution of the special case  $g = \frac{1}{2}$  discussed in this section is consistent with all results inferred in earlier sections from perturbative approaches and scaling, and gives us confidence in their more general validity.

## IX. DISCUSSION AND CONCLUSIONS

In this paper we have seen that electron-electron interactions play a crucial role in determining the nature of transport in one-dimensional structures. In particular, for repulsive interactions we found that an arbitrarily weak barrier in an otherwise infinite Luttinger liquid will cause total reflection of an incident current and hence insulating behavior at zero temperature. The experimental signature for this Luttinger-liquid physics will be the power-law scaling of the conductance as a function of temperature for temperatures larger than the finite-length cutoff energy  $T_L$ . The exponent of this power law is then a measure of the interaction strength of the Luttinger liquid. Moreover, the  $I$ - $V$  characteristics should exhibit a similar power-law behavior with the same exponent.

We have also discussed the nature of resonant tunneling through a double-barrier structure in a Luttinger liquid. We found that there can be perfect resonant transmission, provided the interactions are not too strongly repulsive, or in practice with a Coulomb interaction the electron density not too low. Moreover, at finite but small temperatures the resonance line shapes are described by a universal scaling function. It should be emphasized, however, that in this theory we have ignored any structure within the island between the two barriers. As such, our results are valid only on time scales long compared to  $\tau_{\text{island}}$ , the time which it takes for an electron to traverse the island (or equivalently for temperatures below  $T_{\text{island}} = \hbar/k_B \tau_{\text{island}}$ ). Thus, in a realistic experiment on a one-dimensional wire, we expect the predicted

scaling behavior to be valid for temperature scales between  $T_{\text{island}}$  and  $T_L$ . In general, two parameters must be tuned to achieve a resonance; however, in the case of a symmetric double-barrier structure, resonance may be achieved by tuning a single parameter, such as a gate voltage. For slightly asymmetric barriers, it will nevertheless be possible to observe the resonances at finite temperature; however, as the temperature goes to zero, the peak height of the resonance will go to zero.

In the absence of any barriers, the two-terminal conductance of a pure one-channel 1D wire is given by  $ge^2/h$ . This result, however, should be qualified by the fact that at present we have no theory for the interface between the one-dimensional Luttinger liquid and the two- or three-dimensional (Fermi liquid) leads. The contact resistance between the 1D sample and the leads may well be very important in practice. It should be noted that conductance quantization in units of  $e^2/h$  has been observed for point contacts.<sup>9</sup> In such experiments, though, the one-dimensional channel is very short—containing only a few electrons—so that the three-dimensional leads dominate the behavior. Unfortunately, at present it has not been possible to observe such conductance quantization in longer channels. Presumably this is due to the difficulty of eliminating the effects of impurity scattering in the wire. If clean wires can be made, though, which are long enough that many (say tens) of electrons reside in the length of the 1D segment, then quantization of the conductance in units smaller than  $e^2/h$  would be expected.

The effects of disorder in a one-dimensional channel can be minimized by applying a strong magnetic field. Since this will tend to spatially separate the right- and left-moving electrons, it should reduce the unwanted impurity backscattering. The optimal value of the magnetic field, in order to maximize the spatial separation between right and left movers, corresponds to a magnetic length comparable to the width of the one-dimensional confining potential.

There is a deep connection between the 1D transport which we have studied in this paper and edge transport in the fractional quantum-Hall regime of a two-dimensional electron gas. Indeed, the quantum-Hall regime may well be the best place to observe the phenomena which we have predicted. Specifically, Wen has shown in a recent series of papers<sup>35</sup> that the edge excitations of a two-dimensional electron gas in the fractional quantum-Hall regime may be described as a “chiral Luttinger liquid.” A quantum-Hall bar which is long, but not one dimensional, will consist of chiral Luttinger liquids on each edge which move in opposite directions. This is formally identical to a one-dimensional Luttinger liquid, which has both right- and left-moving electrons. Moreover, as Wen has shown,<sup>35,36</sup> the dimensionless conductance of this Luttinger liquid is simply given by the filling factor of the bulk fractional quantum-Hall state, at least for the odd-integer states  $g = \nu = 1/m$ . Since the two edges are assumed well separated from each other, tunneling between the edges is strongly suppressed. Therefore, the problem of backscattering in the bulk Luttinger liquid is eliminated. Moreover, since it is much easier to fabricate

large two-dimensional electron gases, the cutoff due to the finite system size ( $L$ ) should no longer be a limiting factor, and it should be possible to achieve a much wider range between  $T_{\text{island}}$  and  $T_L$ . Imagine now a constriction in this quantum-Hall “wire” which allows tunneling between the two edges. This is precisely the analogue of the single-barrier problem described in Sec. III, and in a  $\nu = \frac{1}{3}$  state, for instance, the two-terminal conductance should vanish at low temperatures as  $T^{-4}$ . In the presence of two such constrictions, we have precisely the resonant tunneling problem described in Sec. IV. At low temperatures the resonance line shapes should be described by a truly universal scaling function with no undetermined “free” parameter  $g$ . It is also clear that there will be qualitative differences between resonances in the integer and fractional Hall effects, with only the latter having resonant widths which vanish in the zero-temperature limit.

In the absence of a magnetic field, the electron spin degree of freedom will play an important role, and this leads to some novel effects. In particular, we showed that with a barrier present, in addition to the perfectly conducting and perfectly insulating phases, it is possible, under certain conditions, to have a phase which is a charge insulator yet a spin conductor.

In the presence of a double-barrier structure, the resonant tunneling of electrons with spin will be dominated by so-called “Kondo resonances.” In contrast to spinless electron resonances, these resonances occur when the charge between the barriers is an odd integer, and there is a remaining spin degree of freedom on the island. Therefore, in an experiment analogous to that of Meirav *et al.*<sup>8</sup> the resonance peaks should have a periodicity as a function of gate voltage which corresponds to the addition of two electrons to the island.

It is worthwhile to contrast this Kondo resonance in the Luttinger liquid with the analogous resonances in the case where the leads are Fermi liquids. This latter case has been studied recently by a number of authors.<sup>17–19</sup> With Fermi-liquid leads, at low temperatures the Kondo resonance peak has a temperature independent width which is essentially given by the Fermi’s “golden-rule” lifetime for an electron on the island. When the gate voltage is adjusted so that the charge on the island is precisely an odd integer, the resonance peak is exactly centered about the Fermi energy. As the gate voltage is tuned “off valence,” away from this value, the center of the resonance peak shifts away from the Fermi energy. But as long as the barriers are large, in the “Kondo limit,” the charge on the island will depend only very weakly on the gate voltage, and the Fermi energy should still reside within the width of the resonance peak. When the leads are Luttinger liquids, on the other hand, we have seen that the resonance widths vanish at zero temperature, even if the barriers are not large. Then, at  $T=0$ , the resonance will be at the Fermi energy only when the average charge on the island is precisely an odd integer. Since the average charge on the island is a smooth function of the gate voltage (unless the barrier heights are infinite), the resonance in this case will be infinitely sharp as a function of gate voltage. At finite temperatures, the

resonances will have a universal shape, as described in Sec. VII.

Throughout this paper we have assumed that the Coulomb interaction between electrons in the one-dimensional wire is of short range, and have ignored all complications which might arise from the long-ranged piece of the interaction. As we now discuss briefly, the effects of a long-ranged  $1/r$  Coulomb interaction, while possibly leading to qualitative changes in the results, will in practice be hard to detect experimentally, since they will consist primarily of a weak logarithmic temperature and frequency correction. Consider for simplicity the spinless electron gas with long-ranged interactions. One expects that the effective action (2.4) should be modified slightly, with the  $(\nabla\theta)^2$  term replaced by a term of the form  $\int dk k^2 U(k) |\theta(k)|^2$ , where  $U(k)$  is the Fourier transform of the Coulomb interaction. For a  $1/r$  interaction this gives  $U(k) \approx -\ln(k)$  in one dimension. The effective quadratic action would then describe a density wave with a modified dispersion of the form  $\omega \approx \sqrt{-\ln(k)}k$ , rather than the purely linear dispersion for short-ranged interactions. Because this logarithmic term varies so weakly with distance, we expect that it will have a rather weak effect on the results for transport through barriers, leading initially to weak logarithmic temperature corrections. In the asymptotic zero-temperature limit, though, these corrections can become large and may change the results even qualitatively. Indeed, even in the absence of a barrier,  $1/r$  Coulomb interactions have been argued to destabilize the Luttinger liquid at very low temperatures. Specifically, in Ref. 37, it was shown that a  $1/r$  interaction leads to an unbinding of space-time vortices (in the  $\phi$  field), which destroy the fluid phase, probably forming a Wigner crystal with long-ranged crystalline correlations at  $T=0$ . Strictly speaking, though, a correct analysis must also incorporate the transverse pieces of the Coulomb interaction (i.e., retardation effects due to the dynamics of the photon) which were ignored in the aforementioned analysis. The ultimate fate of the Luttinger liquid at the longest length scales and  $T=0$  in this case is presently, as far as we know, a theoretically open question.

Theoretically, there is a deep connection between much of the analysis in this paper, and the recent problem of defects in quantum-spin chains,<sup>38</sup> and more generally with boundary or surface critical phenomena in two-dimensional theories at their critical point.<sup>39</sup> This connection is clearest from the analysis in Sec. VIII, where a model of a Luttinger liquid with barrier was first mapped into a quantum spin chain with boundary field, and eventually into the 2D Ising model at its critical point with a boundary magnetic field. Physically, the 1D Luttinger liquid, when viewed as a 2D theory in space time, describes a 2D critical theory. A defect or weak link in the 1D wire becomes a surface or defect line in the effective 2D theory. The conductance through the weak link, which is a dimensionless number when expressed in units of  $e^2/h$ , characterizes the surface critical phenomena in the 2D theory. The generic case of total reflection or perfect transmission through the weak link corresponds to an open or closed boundary, respectively, in

the 2D critical theory. However, the new critical points we found in the spinful case in Secs. V and VI (and shown in Figs. 8 and 11) which had a nontrivial yet universal conductance, presumably correspond to nontrivial surface or boundary critical phenomena in the underlying 2D critical theory. It is quite possible that the powerful methods of conformal field theory might be applied here to give nonperturbative values of the exponents and other universal critical properties.

#### ACKNOWLEDGMENTS

It is a pleasure to thank I. Affleck, V. Chandrasaekar, D. Divincenzo, S. M. Girvin, L. I. Glazman, D. A. Huse, P. A. Lee, H. Mooij, R. Webb, and X. G. Wen for invaluable discussions. We would also like to acknowledge the Institute for Theoretical Physics in Santa Barbara, where part of this work was carried out.

#### APPENDIX A: PERTURBATION THEORY

In this appendix we outline the perturbative calculations of the conductance and  $I$ - $V$  characteristics for transport through a single barrier in the limits of a small hopping  $t$  and for small backscattering  $v(2k_F)$ . We compute the current in the presence of an arbitrary voltage at temperature  $T$  to lowest nontrivial order in perturbation theory.

We begin with the small-hopping limit, which is most conveniently expressed in the  $\phi$  representation. In the presence of an externally applied voltage the partition function may be written

$$Z = \int D[\phi] e^{-S[\phi]}, \quad (\text{A1})$$

where

$$S[\phi] = g \sum_{i\omega_n} |\omega_n| |\phi(\omega_n)|^2 + \sum_n t_n \int_0^\beta d\tau \cos[2n\sqrt{\pi}\phi(\tau) + na(\tau)], \quad (\text{A2})$$

where the voltage in real time is given by  $V(t) = \partial_t a(t)$ . Here  $t_n$  corresponds to the hopping of  $n$  (spinless) electrons across the weak link. If we expand the partition function in powers of  $t$ , we may integrate out  $\phi$ :

$$Z = Z_0 \left[ 1 + \frac{1}{4} \sum_n t_n^2 \int_0^\beta d\tau_1 d\tau_2 \cos\{n[a(\tau_1) - a(\tau_2)]\} \times P_{2n^2/g}(\tau_1 - \tau_2) \right], \quad (\text{A3})$$

where  $Z_0$  is the partition with  $t=0$  and

$$P_{2n^2/g}(\tau) \equiv \langle T_\tau e^{i2n\sqrt{\pi}[\phi(\tau) - \phi(0)]} \rangle_0 = \left[ \frac{\pi\tau_c/\beta}{\sin(\pi\tau/\beta)} \right]^{2n^2/g}. \quad (\text{A4})$$

Here  $\tau_c \approx E_F^{-1}$  is a short-time cutoff. The current may then be calculated via  $I(\tau) = \delta \ln Z / \delta a(\tau)$ . We then analytically continue to real time by distorting the contour of the  $\tau$  integral from 0 to  $\beta$  to run from  $t' = -\infty$  to

$t' = t$  and then back to  $-\infty + i\beta$ .<sup>40</sup> We then find

$$I(t) = \frac{1}{2} \sum_n t_n^2 \int_{-\infty}^t dt' \sin\{n[a(t) - a(t')]\} \times \frac{P_{2n^2/g}^>(t-t') - P_{2n^2/g}^<(t-t')}{i}, \quad (\text{A5})$$

where  $P^{>(<)}(t)$  is the analytic continuation  $P[\tau \rightarrow +(-)it]$ . From this we may compute the current at constant dc voltage and the (linear) conductance (restoring the approximate factors of  $e$  and  $\hbar$ ):

$$I(V) = \frac{e^2}{h} \pi \sum_n n t_n^2 \frac{P_{2n^2/g}(nV) - P_{2n^2/g}(-nV)}{2i}, \quad (\text{A6a})$$

$$G(\omega) = \frac{e^2}{h} \pi \sum_n n^2 t_n^2 \frac{P_{2n^2/g}(\omega)}{i\omega}, \quad (\text{A6b})$$

where

$$P_\lambda(E) = \int_0^\infty dt (e^{iEt} - 1) \frac{P_\lambda^>(t) - P_\lambda^<(t)}{i}. \quad (\text{A7})$$

This integral may be evaluated in the  $\omega=0$  and  $T=0$  limits,

$$P_\lambda(E, T=0) = i\tau_c (E\tau_c)^{\lambda-1} [f_1(\lambda) + if_2(\lambda)], \quad (\text{A8a})$$

$$P_\lambda(E \rightarrow 0, T) = iE\tau_c^2 (\tau_c T)^{\lambda-2} f_3(\lambda), \quad (\text{A8b})$$

where

$$f_1(\lambda) = \frac{\pi}{\Gamma(\lambda)}, \quad (\text{A9a})$$

$$f_2(\lambda) = \frac{\pi}{\Gamma(\lambda)} \tan \frac{\pi}{2} \lambda, \quad (\text{A9b})$$

$$f_3(\lambda) = \frac{\pi^{\lambda-1}}{2} \frac{\Gamma(\frac{1}{2})\Gamma(\lambda/2)}{\Gamma(\frac{1}{2} + (\lambda/2))}. \quad (\text{A9c})$$

In terms of these functions we may express the coefficients  $b$  which appear in Eq. (3.12) as

$$b_{nT} = \pi n^2 f_3(\lambda), \quad (\text{A10a})$$

$$b_{n\omega} = \pi n^2 [f_1(\lambda) + if_2(\lambda)], \quad (\text{A10b})$$

$$b_{nV} = \pi n^\lambda f_2(\lambda), \quad (\text{A10c})$$

evaluated at  $\lambda = 2n^2/g$ . With spin the analysis is similar, and we find for the coefficients  $d$ , appearing in Eq. (5.11), the result

$$d_T(n_\sigma, n_\rho) = \frac{\pi}{2} n_\rho^2 f_3(\lambda), \quad (\text{A11a})$$

$$d_\omega(n_\sigma, n_\rho) = \frac{\pi}{2} n_\rho^2 [f_1(\lambda) + if_2(\lambda)], \quad (\text{A11b})$$

$$d_V(n_\sigma, n_\rho) = \frac{\pi}{2} n_\rho^\lambda f_1(\lambda), \quad (\text{A11c})$$

evaluated at  $\lambda = 2n_\rho^2/g_\rho + 2n_\sigma^2/g_\sigma$ .

In the opposite limit of small barriers, the action in the  $\theta$  representation for spinless electrons is

$$\begin{aligned}
S[\theta] &= \frac{1}{g} \sum_{i\omega_n} |\omega_n| |\theta(\omega_n)|^2 \\
&+ \sum_n v_n \int_0^\infty d\tau \cos[2n\sqrt{\pi}\theta(\tau)] \\
&+ \frac{1}{\sqrt{\pi}} \int_0^\beta d\tau ia(\tau) \partial_\tau \theta(\tau), \quad (\text{A12})
\end{aligned}$$

where again in real time  $V(t) = \partial_t a(t)$ . By changing variables  $\theta(\tau) \rightarrow \theta(\tau) + ga(\tau)/2\sqrt{\pi}$ , this can be written in a more tractable form,

$$\begin{aligned}
S &= \sum_{i\omega_n} \frac{1}{g} |\omega_n| |\theta(\omega_n)|^2 + \frac{g}{4\pi} |\omega_n| |a(\omega_n)|^2 \\
&+ \sum_n v_n \int_0^\beta d\tau \cos[2n\sqrt{\pi}\theta(\tau) - nga(\tau)]. \quad (\text{A13})
\end{aligned}$$

A similar expansion in powers of  $a(\tau)$  and analytic continuation leads to

$$\begin{aligned}
I(V) &= \frac{e^2}{h} V \left[ g - \pi \sum_n ng |v_n|^2 \right. \\
&\quad \left. \times \frac{P_{2n^2g}(ngV) - P_{2n^2g}(-ngV)}{2iV} \right] \quad (\text{A13a})
\end{aligned}$$

and

$$G(\omega) = \frac{e^2}{h} \left[ g - \pi \sum_n (ng)^2 |v_n|^2 \frac{P_{2n^2g}(\omega)}{\omega} \right]. \quad (\text{A13b})$$

The coefficients  $a$  appearing in Eq. (3.5) are then

$$a_{nT} = \pi(ng)^2 f_3(\lambda), \quad (\text{A14a})$$

$$a_{n\omega} = \pi(ng)^2 [f_1(\lambda) + if_2(\lambda)], \quad (\text{A14b})$$

$$a_{nV} = \pi(ng)^\lambda f_1(\lambda), \quad (\text{A14c})$$

evaluated at  $\lambda = 2n^2g$ . Similarly, with spin, the coefficients  $c$  appearing in (5.6) are given by

$$c_T(n_\sigma, n_\rho) = \frac{\pi}{2} (n_\rho g_\rho / 2)^2 f_3(\lambda), \quad (\text{A15a})$$

$$c_\omega(n_\sigma, n_\rho) = \frac{\pi}{2} (n_\rho g_\rho / 2)^2 [f_1(\lambda) + if_2(\lambda)], \quad (\text{A15b})$$

$$c_V(n_\sigma, n_\rho) = \frac{\pi}{2} (n_\rho g_\rho / 2)^\lambda f_1(\lambda), \quad (\text{A15c})$$

evaluated at  $\lambda = n_\rho^2 g_\rho / 2 + n_\sigma^2 g_\sigma / 2$ .

## APPENDIX B: RENORMALIZATION GROUP FOR DOUBLE BARRIERS

In this appendix, we sketch the real-space renormalization-group procedure used to derive the flow equations (4.5). We consider spinless electrons in the general situation where we have an island coupled to two leads with asymmetric hopping strengths  $t_+$  and  $t_-$ . By classifying the different kinds of hops in terms of the charges  $q_i = \Delta Q_+ - \Delta Q_-$  and  $r_i = \Delta Q_{\text{dot}}$ , the partition function in the Coulomb plasma representation may be written

$$\begin{aligned}
Z &= \sum_n \sum_{q_i} t_+^{\sum_i (1+q_i r_i)/2} t_-^{\sum_i (1-q_i r_i)/2} \\
&\quad \times \int_0^\beta d\tau_{2n} \cdots \int_0^{\tau_2} d\tau_1 \exp \left[ - \sum_{i < j} V_{ij} \right], \quad (\text{B1})
\end{aligned}$$

$$\begin{aligned}
V_{ij} &= \frac{1}{2g} [q_i q_j + K_1 r_i r_j \\
&\quad + K_2 (r_i q_j + r_j q_i)] \ln(\tau_i - \tau_j) / \tau_c,
\end{aligned}$$

where  $\tau_c \approx E_F^{-1}$  is a short-time cutoff. This expression is a generalization of that given for the symmetric case in (4.4). In (B1) the sums run over all possible configurations of charges such that  $r_i$  alternates in time and  $\sum_i q_i = \sum_i r_i = 0$ . The initial values of  $K_1$  and  $K_2$  are 1 and 0, respectively; however, as we shall see, their values flow in the renormalization group. The lead conductance  $g$ , on the other hand, is not renormalized.

We now analyze the above model using the real-space perturbative renormalization-group method invented by Anderson, Yuval, and Hamann. This procedure involves first decimating closely spaced dipole charges separated by a distance between  $\tau_c$  and  $\tau_c + d\tau_c$ . Then we rescale  $\tau$  to restore the original cutoff.

If the dipole is between charges  $\tau_i$  and  $\tau_{i+1}$ , then its interaction with the rest of the charges is

$$\sum_j \frac{1}{2g} [qq_j + K_1 rr_j + K_2 (rq_j + qr_j)] \tau_c \partial_\tau \ln(\tau - \tau_j) / \tau_c. \quad (\text{B2})$$

The constraint on the ordering of the  $r$ 's specifies that  $r = r_i$ . For a virtual hop into the + lead,  $q = +r_i$ , whereas for a virtual hop into the - lead,  $q = -r_i$ . By expanding the exponential and integrating out dipoles with separation between  $\tau_c$  and  $\tau_c + d\tau_c$ , the partition function can be expressed as

$$Z = Z' \left[ 1 + \sum_{i,j} d\tau_c \int_{\tau_i}^{\tau_{i+1}} d\tau \left[ \frac{t_+^2 + t_-^2}{2g} (K_1 r_i r_j + K_2 r_i q_j) + \frac{t_+^2 - t_-^2}{2g} (r_i q_j + K_2 r_i r_j) \right] \tau_c \partial_\tau \ln(\tau - \tau_j) / \tau_c \right]. \quad (\text{B3})$$

Note that there is no term involving  $q_i q_j$ , which follows from the fact that  $q_i$  is free to be  $\pm 1$ . We may now reexponentiate (B3) and rewrite the partition function in the form of (B1), with new parameters  $K'_1$  and  $K'_2$ .

Finally, to complete the RG transformation we rescale  $\tau \rightarrow e^l \tau'$  with  $l = d\tau_c / \tau_c$ . Noting that  $\sum_{i < j} r_i r_j = \sum_{i < j} q_i q_j = -\frac{1}{2} \sum_i 1$  and  $\sum_{i < j} r_i q_j + q_i r_j = -\sum_i q_i r_i$ , we may then compute the renormalization of  $t_+$  and  $t_-$ .



The resulting flow equations are

$$dK_1/dl = -4\tau_c^2[K_1(t_+^2 + t_-^2) + K_2(t_+^2 - t_-^2)], \quad (\text{B4a})$$

$$dK_2/dl = -2\tau_c^2[K_2(t_+^2 + t_-^2) + (t_+^2 - t_-^2)], \quad (\text{B4b})$$

$$dt_{\pm}/dl = [1 - (1 + K_1 \mp 2K_2)/4g]t_{\pm}. \quad (\text{B4c})$$

For a symmetric double barrier,  $t_+ = t_- = t$ , we have  $K_2 = 0$ , and these equations simplify to the equations presented in (4.5). For the case of electrons with spin, the flow equations for the Kondo resonance (6.4) may be derived in an analogous fashion.

- 
- <sup>1</sup>J. G. Bednorz and K. A. Muller, *Z. Phys. B* **64**, 188 (1986).  
<sup>2</sup>P. W. Anderson, *Science* **235**, 1196 (1987); *Phys. Rev. Lett.* **64**, 1839 (1990).  
<sup>3</sup>J. M. Luttinger, *J. Math. Phys.* **15**, 609 (1963).  
<sup>4</sup>A. Luther and L. J. Peschel, *Phys. Rev. B* **9**, 2911 (1974); *Phys. Rev. Lett.* **32**, 992 (1974); A. Luther and V. J. Emery, *ibid.* **33**, 589 (1974).  
<sup>5</sup>J. Solyom, *Adv. Phys.* **28**, 201 (1970); V. J. Emery, in *Highly Conducting One-Dimensional Solids*, edited by J. T. Devreese (Plenum, New York, 1979).  
<sup>6</sup>F. D. M. Haldane, *J. Phys. C* **14**, 2585 (1981).  
<sup>7</sup>F. D. M. Haldane, *Phys. Rev. Lett.* **47**, 1840 (1981).  
<sup>8</sup>U. Meirav, M. A. Kastner, M. Heiblum, and S. J. Wind, *Phys. Rev. B* **40**, 5871 (1989).  
<sup>9</sup>G. Timp, in *Mesoscopic Phenomena in Solids*, edited by B. L. Altshuler, P. A. Lee, and R. A. Webb (Elsevier, Amsterdam, 1990).  
<sup>10</sup>R. Landauer, *Philos. Mag.* **21**, 863 (1970); M. Buettiker, *Phys. Rev. Lett.* **57**, 1761 (1986).  
<sup>11</sup>D. B. Averin and K. K. Likharev, *J. Low Temp. Phys.* **62**, 345 (1986); E. Ben-Jacob, D. J. Bergman, B. J. Matkowsky, and Z. Schuss, *Phys. Rev. B* **34**, 1572 (1986).  
<sup>12</sup>For a recent review of the Coulomb blockade and related phenomena, see D. V. Averin and K. K. Likharev, in *Mesoscopic Phenomena in Solids* (Ref. 9).  
<sup>13</sup>H. van Houten and C. W. J. Beenakker, *Phys. Rev. Lett.* **63**, 1893 (1989).  
<sup>14</sup>Y. Meir, N. S. Wingreen, and P. A. Lee, *Phys. Rev. Lett.* **66**, 3048 (1991).  
<sup>15</sup>C. L. Kane and M. P. A. Fisher, *Phys. Rev. Lett.* **68**, 1220 (1992).  
<sup>16</sup>C. L. Kane and M. P. A. Fisher, *Phys. Rev. B* **46**, 7268 (1992).  
<sup>17</sup>T. K. Ng and P. A. Lee, *Phys. Rev. Lett.* **61**, 1768 (1988).  
<sup>18</sup>L. I. Glazman and M. E. Raikh, *Pis'ma Zh. Eksp. Teor. Fiz.* **47**, 378 (1988) [*JETP Lett.* **47**, 452 (1988)].  
<sup>19</sup>N. S. Wingreen, Y. Meir, and P. A. Lee (private communication).  
<sup>20</sup>T. Giamarchi and H. J. Schultz, *Phys. Rev. B* **37**, 325 (1988).  
<sup>21</sup>D. S. Fisher and P. A. Lee, *Phys. Rev. B* **23**, 6851 (1981).  
<sup>22</sup>W. Apel and T. M. Rice, *Phys. Rev. B* **26**, 7063 (1982).  
<sup>23</sup>L. I. Glazman, I. M. Ruzin, and B. I. Shklovskii, *Phys. Rev. B* **45**, 8454 (1992).  
<sup>24</sup>P. W. Anderson, G. Yuval, and D. R. Hamann, *Phys. Rev. B* **1**, 4464 (1970).  
<sup>25</sup>J. M. Kosterlitz and D. J. Thouless, *J. Phys. C* **6**, 1181 (1981).  
<sup>26</sup>A. O. Caldeira and A. J. Leggett, *Ann. Phys. (N.Y.)* **149**, 374 (1983).  
<sup>27</sup>A. Schmid, *Phys. Rev. Lett.* **51**, 1506 (1983); F. Guinea, V. Hakim, and A. Muramatsu, *ibid.* **54**, 263 (1985); M. P. A. Fisher and W. Zwerger, *Phys. Rev. B* **32**, 6190 (1985).  
<sup>28</sup>S. M. Girvin, L. I. Glazman, M. Jonson, D. R. Penn, and M. D. Stiles, *Phys. Rev. Lett.* **64**, 3183 (1990).  
<sup>29</sup>M. H. Devoret, D. Esteve, H. Grabert, G.-L. Ingold, H. Pothier, and C. Urbina, *Phys. Rev. Lett.* **64**, 1824 (1990).  
<sup>30</sup>A. Furusaki and N. Nagaosa (unpublished).  
<sup>31</sup>J. Kondo, *Prog. Theor. Phys.* **32**, 37 (1964).  
<sup>32</sup>F. Guinea, *Phys. Rev. B* **32**, 7518 (1985).  
<sup>33</sup>J. B. Kogut, *Rev. Mod. Phys.* **51**, 659 (1979).  
<sup>34</sup>E. L. Lieb, T. Schultz, and D. Mattis, *Ann. Phys. (N.Y.)* **16**, 407 (1961).  
<sup>35</sup>X. G. Wen, *Phys. Rev. B* **43**, 11 025 (1991); *Phys. Rev. Lett.* **64**, 2206 (1990).  
<sup>36</sup>X. G. Wen, *Phys. Rev. B* **44**, 5708 (1991).  
<sup>37</sup>M. P. A. Fisher and G. Grinstein, *Phys. Rev. Lett.* **60**, 208 (1988).  
<sup>38</sup>I. Affleck (unpublished).  
<sup>39</sup>J. L. Cardy, *Nucl. Phys. B* **240**, 514 (1984); *Adv. Studies Pure Math.* **19**, 127 (1989).  
<sup>40</sup>J. Rammer and H. Smith, *Rev. Mod. Phys.* **58**, 323 (1986).

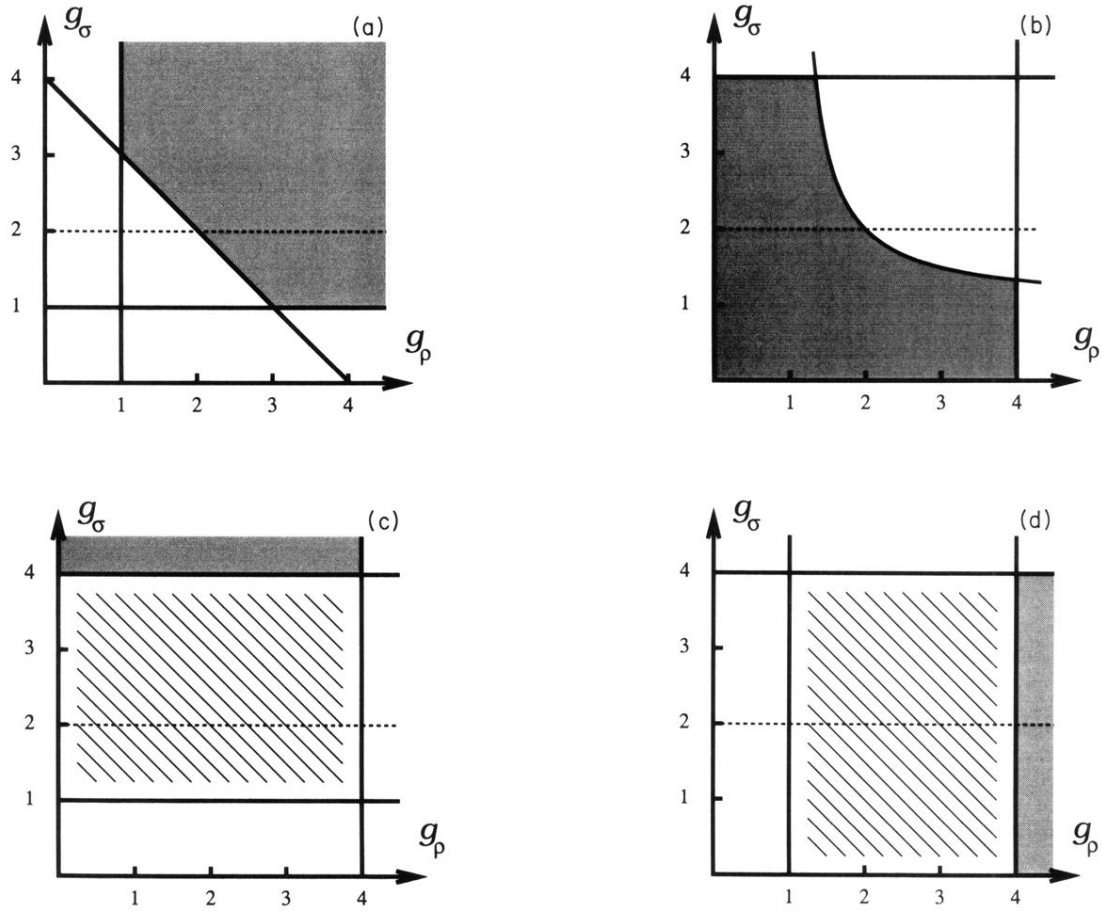


FIG. 6. Regions of stability of various phases of the interacting electron gas with spin, incident upon a single barrier, shown in the  $g_p$ - $g_\sigma$  plane: (a) The shaded region corresponds to the phase in which both spin and charge are perfectly transmitted, and was obtained in the limit of weak backscattering, Eq. (5.5). (b) Shaded region corresponds to the phase in which both charge and spin are completely reflected, obtained in the limit of large barriers from Eq. (5.10). (c) Shaded region corresponds to the phase which is a spin conductor and/or charge insulator, as discussed in Sec. V C. (d) Shaded region is a phase which is a charge conductor and/or spin insulator. In (c) and (d) the cross-hatched regions indicate stability of the respective “mixed” phases in the case of a barrier with inversion symmetry. In each of the figures the dashed line at  $g_\sigma = 2$  corresponds to a spinful electron gas with SU(2) spin symmetry.